Researching the Properties of a 3D-Printed Living Material Containing *C. reinhardtii*

J.T.E. Beets
Department of Bionanoscience
Faculty of Applied Sciences
Delft University of Technology

Supervisor: Dr. M. -E. Aubin-Tam

Assessment committee:
Dr. M. -E. Aubin-Tam
Dr. T. Idema
Dr. K. Masania
C. Wehrmann

A thesis submitted to obtain the degree of Master of Science in Nanobiology

August 2023, Delft

Summary

Incorporating living cells into a non-living matrix is one of the many possible steps that can be undertaken to stop climate change. Especially, photosynthetic organisms have a promising future in material design as they can capture atmospheric carbon dioxide and 'breathe' oxygen. This research dives into unravelling the properties of a hydrogel-based living material containing *C. reinhardtii*.

To facilitate a systematic exploration, this goal was divided into three smaller pieces. Firstly, the study delves into the mechanical characteristics, aiming to identify the most suitable bio-ink crosslink technique and composition. To validate the mechanical properties the living material was subjected to rheology and a bridging test. Concluded can be that crosslinking and algae growth improve the mechanical stability of the material, whereas, gelatin did not. The sagging behaviour of the material looked promising.

Secondly, the photosynthetic activity of this living material was researched. It was found that the rise of O_2 levels can not be measured accurately, the non-living matrix can release a high amount of CO_2 of over 20.000 ppm and airtightness poses a complex challenge in this field of research.

Lastly, the project incorporates attempts to find effective techniques for studying the livingness of this unique material. In this part of the research, inverted optical microscopy, 3D laser scanning microscopy and chlorophyll extraction were discarded as suitable methods to study the livingness of the algae material. It was proven that leveraging the autofluorescence of the algal chlorophyll confocal laser scanning microscopy gives high-resolution images and the livingness of this living material could be studied with this technique in the near future.

This research significantly contributes to our understanding of this hydrogel-based living material and its many challenging properties. It underscores the importance of innovative materials like these in addressing contemporary environmental challenges, particularly in carbon capture. Moreover, it highlights the complexity of characterizing such materials, paving the way for further exploration and development in this relatively new field.

Contents

Chapter 1

Introduction

1.1 Research Relevance

In an era defined by the pressing concerns of global climate change, the necessity to seek innovative and sustainable solutions has taken center stage. Humanity is at a crossroads due to the tremendous problems caused by environmental deterioration as well as the rising need for resources and energy. The search for novel materials and resources capable of addressing these issues has evolved from a purely scientific pursuit into a moral obligation as we embrace environmental responsibility and technological advancement.

Climate change, an undeniable consequence of human activity, affects every aspect of our lives since it has numerous negative effects on ecosystems, the economy, and people's well-being[1;2;3;4]. International legislation, corporate initiatives, and individual activities all reflect the necessity to reduce greenhouse gas emissions, halt biodiversity loss, and adopt sustainable practices[5;6;7]. Next to this, the role of innovative research plays an important role in this dynamic.

This research takes its relevance from this broader context. The exploration of engineered living materials (ELMs) as sustainable materials offers a potential solution to one of the most prominent challenges of our time: reducing atmospheric carbon dioxide levels[8]. Strategic studying and fabrication of ELMs, that incorporate organisms that capture CO_2 through photosynthesis, is one of the potential solutions to this problem[9;10;11;12]. By researching the mechanical and photosynthetic properties of a biodegradable bio-ink that incorporates eukaryotic microalgae into its matrix, this study seeks to advance our understanding of the effects of climate change. The study of this ELM will lead to a deeper comprehension of how ELMs might assist in meeting the demand for high-performance, renewable and carbon-capturing materials.

1.2 Engineering Living Materials

In the context of addressing climate change, this section elaborates on two important aspects of the practice of engineering living materials. The first aspect emphasizes the urgency of creating sustainable alternatives to combat plastic pollution, highlighting the pressing need to reduce our reliance on traditional plastics. The second aspect underscores the significance of harnessing the carbon-capturing capabilities of algae, offering a potential solution to curbing atmospheric carbon dioxide levels, a pivotal goal in the battle against climate change. These two facets underscore the mission of the overarching research: to engineer materials that align with a sustainable and environmentally responsible future.

1.2.1 Biodegradable Material Design

One of the factors that impacts climate change is the growing demand for bulk materials. This upsurge in demand results in the accumulation of plastic waste. Currently, the global annual production of plastic waste amounts to approximately 400 million tons[13]. This waste ends up in, for example, oceans in the form of microplastics and these microplastics are detrimental to the ecosystems of the ocean[14]. A study conducted by Li et al. (2020), illustrates the impact of microplastics on *C. reinhardtii*, a freshwater microalgae species. The results show that high microplastic concentrations significantly inhibited growth, caused physical blockage, cytotoxicity, and membrane damage, hindered cell settlement and negatively impacted the photosynthetic activity of the algae[15]. The substitution of plastics with biodegradable, durable and sustainable materials presents the solution to resolve the issue of plastic waste. A branch in this circular movement of Biodesign is the development of bio-inks for 3D printing ELMs[16].

The focus of this research lies on a hydrogel-based material consisting of Microcrystalline Cellulose (MCC), κ-Carrageenan, sodium alginate, agar and Tris minimal solution. Agar and κ-Carrageenan are natural polymers derived from red marine algae and sodium alginate is an alginic salt and copolymer obtained from the cell walls of brown algae[17]. On one hand, alginate, agar, and κ-Carrageenan increase the viscosity of the bio-ink, on the other hand, contribute these natural components to the design of a biodegradable material. The MCC fibers, mostly obtained from waste biomass, are biodegradable reinforcing fillers in the polymer blend due to their low cost, low density, non-toxicity and re-usability[18;19].

The engineering of living materials takes the shift to a greener future even further by not only incorporating biodegradable components but also living organisms in the material[16].

1.2.2 Carbon Capturing with Algae

Living materials are bio-hybrid structures with a non-living synthetic matrix as its foundation and the incorporation of biological living cells[20;21;22]. Examples of such synthetic bases include organic or inorganic polymers. The incorporation of

living organisms into a non-living material has several advantages. As explained in the review by Nguyen et al. (2018), living organisms, such as bacteria, algae or fungi cells, have the potential to add additional functionalities to a non-living matrix of bulk material[16]. The added characteristics can range from self-healing to antibiotic secretion or photosynthetic properties. Furthermore, the fabrication of ELMs opens up innovative application opportunities, such as biosensors, smart textiles, fermentation bioreactors and robotics[23;22]. Another benefit of ELMs lies in the capability to employ environmentally-friendly chemistry to produce the components needed for these advanced materials[24].

In short, the broad array of biological pathways, including photosynthesis, sense-and-respond pathways, and self-healing mechanisms present in living cells and organisms, enable the development of a large variety of useful ELMs. Consequently, these engineered living materials harbour tremendous potential in supporting and creating breakthroughs in various application fields.

As mentioned in Section 1.1, this study will leverage the photosynthetic properties of algae. Algae are a diverse group of organisms, with around 70 thousand species they contribute to at least 50% of total carbon fixation globally[25;26;27].

In this research project, *Chlamydomonas reinhardtii*, a strain of microalgae, is used as the living component in a hydrogel-based material. The photosynthetic activity of this microorganism is especially interesting when added to a non-living material as the living material can then convert one of the biggest greenhouse gasses (CO_2) to oxygen. Thus, next to developing a biodegradable material, this new living material can also purify polluted air originating from, for example, high-emitting production processes (e.g. the production of plastics)[8;28;29].

C. reinhardtii exhibits three metabolic pathways, specifically the photoautotrophic, the heterotrophic and the photomixotrophic growth pathways. The former pathway occurs in the presence of UV light and requires CO_2 as the primary carbon source, whereas the second pathway is initiated in the absence of light and depends on alternate carbon sources, such as acetate. The photomixotrophic pathway is a combination of the first two growth behaviours[30].

To exploit the photosynthetic properties as much as possible, it was preferred to study the living material under photoautotrophic circumstances in this research. To achieve this, the algae could only use light to take CO_2 and convert it to glucose and oxygen. This was accomplished by preparing the algal stock and the hydrogel-based bio-ink in a Tris minimum medium. The *C. reinhardtii* algae then grow and multiply through photosynthesis, and the photosynthesis equation is as follows:

$$6CO_2 + 6H_2O + \text{light energy} \rightarrow C_6H_{12}O_6 + 6O_2 \tag{1.1}$$

When measured in an airtight container, the CO_2 and O_2 levels of the living material are expected to show a waving motion. During the light phase, the O_2 level rises while the CO_2 level falls, and vice versa during the dark period. The overall CO_2 level is predicted to drop over time as the algae cells use up the carbon from the air.

1.3 Relevance of 3D printing

With over 12,000 publications last year, 3D printing became one of the most well-known inventions of the past few decades[31]. Even though Dr. Hideo Kodama invented the 3D printer in 1981, it only gained real popularity around 2010[32]. With its open-source community and user-friendliness 3D printing is efficient and straightforward. Furthermore, with printers suitable for both hobbyists to researchers in the ELM field, printer prices range from 90 to 9.200 euros[33]. This makes 3D printing scalable in terms of user type and offers a cost-efficient fabrication strategy for conducting research on printing with living materials.

In addition to this, 3D printing offers a broad variety of geometrical designs as well as structural and functional complexity[34;35;22]. However, there are a few requirements when printing with a 3D printer. Firstly, the bioink should have adequate viscosity to allow the printing of these complex structures and after printing, the bio-ink has to quickly harden to keep the geometry of the printed shape[36]. The bio-ink used in this research project was developed to have a viscosity suitable for 3D printing. After printing, the crosslinking step strengthens the material without harming the algae inside the ELM.

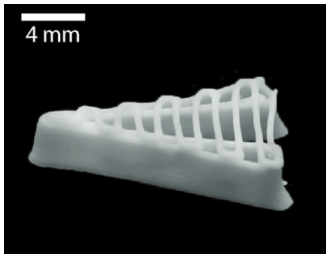

Figure 1.1: Overhang testing of a paste, adapted from Kleger et al. (2019)[37].

Due to the high variety of dimensions, as shown in Figure 1.1, 3D printing offers the opportunity to efficiently look into the multi-faceted aspects of this engineered living material. As a result, this research will look into the effect of the crosslinking step on the mechanical characteristics of the bio-ink, as well as, the photosynthetic activity of the algae inside the ELM and the livingness of the 3D prints containing *C. reinhardtii*.

1.4 Research Outline

This master's research project will carry on the investigation started by Balasubramanian et al. (2021) and Vriend (2021)[24;12]. The main goal of this research project, as presented in the proposal of this thesis[38], is to characterise the photosynthetic activity and mechanical properties of the 3D-printed living microalgal material, developed during the master thesis project of Vivian Vriend[12]. Next to this, the first steps were made to study the livingness and structure of the material.

The main research question put forth is the following:

What are the photosynthetic activity, the livingness and mechanical properties of a hydrogel-based living material containing *C. reinhardtii*?

In order to answer this main research question, it is divided into three sub-questions. To better comprehend the mechanical characteristics and what influences them, consider the first sub-question:

What bio-ink treatment and composition gives the best mechanical properties without becoming detrimental to the living material?

The second sub-question will be related to the photosynthetic activity of the living material and is as follows:

What is the carbon-capturing potential of the living material containing *C. reinhardtii*?

The third sub-question was included later in the project and is stated below:

What techniques can be used to study the livingness of the living material?

The mechanical properties were researched with two different techniques. First, the 3D-printed material was put through rheology tests. This was done to evaluate the effect of crosslinking duration and concentration, the age of the sample and the presence of algae on the material flow properties. Next, an overhang test was conducted to study the sagging behaviour in order to further understand the mechanical properties of the ELM rheology. To answer the second sub-question, the setup for measuring O_2 or CO_2 must be as airtight and clean as possible. To overcome these challenges, several setups were tested. Inverted optical microscopy and 3D laser scanning microscopy were tested on the sample to learn more about the imaging methods that may be utilized to analyze the structure and livingness of the material. Then attempts at chlorophyll extraction were performed before settling on confocal laser scanning microscopy, leveraging the autofluorescence of chlorophyll in the ELM's algal cells.

All research was done at the Aubin-Tam laboratory and in association with the Shaping Matter lab, at Delft University of Technology. Furthermore, this master's thesis report was written to obtain the degree of Master of Science in Nanobiology and was jointly written as part of the double degree together with the Master Communication Design for Innovation.

Chapter 2

Research Methods

2.1 Algae Bio-Ink

The algae bio-ink used in the research conducted during this thesis was adapted from the thesis research performed by Vriend[12]. As mentioned before, micro-algae were added to the ink to create an algae bio-ink with photosynthetic properties. Aside from this 'original' algae bio-ink, another algae bio-ink with gelatin was developed and researched.

2.1.1 *C. reinhardtii* Stock Preparation

The microalgae used in this research project were of the species *Chlamydomonas reinhardtii*, strain CC-125(mt^+). From a general stock, isolated cultures were grown in Petri dishes with a TAP agar base, to do this the aseptic technique was used. These plates were stored conforming to the setup described by Vriend[12]. After two weeks, one colony was transferred with an inoculation loop to an autoclaved Erlenmeyer containing 100 mL Tris minimal solution (Tris) and a tube connected to two sterile air filters for sterile airflow[24]. This was done in a flow cabinet. The Erlenmeyer was then stored statically for one week in a box[12].

2.1.2 Original Bio-Ink

To prepare 200 mL of the original bio-ink, 6 g of VIVAPUR's Microcrystalline Cellulose and Sodium Carboxymethylcellulose mix (MCC) was added to 200 mL Tris in a large beaker. This was done on a bench equipped with a Bunsen burner to allow for a clean work environment. The suspension was mixed for 5 minutes with a handheld kitchen blender (Blokker BL-11302), resulting in a smooth, white mixture with a density resembling Ketchup. After letting this mixture sit on the bench for 15 minutes[22], 3 g of κ-Carrageenan was added, then 3 g of sodium alginate and lastly 3 g of agar, each mixed for 2 minutes before adding the next ingredient. After mixing in the agar, the mixture should have the appearance of a vast paste resembling the density of thick honey. The beaker was then sealed with aluminium foil and tape and sent to be autoclaved. After autoclaving, the final bio-ink was stored at 30 °C for two days.

2.1.3 Gelatin Bio-ink

To make bio-ink with gelatin, first 2 g gelatin powder was added to 200 mL Tris minimal solution and mixed with the handheld kitchen blender in a large beaker. After this, 6 g of MCC was added and the suspension was mixed for 5 minutes with the same blender to form a thick liquid resembling Ketchup. Then the mixture was allowed to settle for 15 minutes[22] in a 37 °C room or cabinet. After this step, the same protocol was followed as described in section 2.1.2, starting from the step where κ-Carrageenan was added to the mixture. The final bio-ink with gelatin was stored at 30 °C for two days.

2.1.4 Algae Bio-Ink and Print Preparation

To prepare the (algae) bio-ink for 3D printing, the 2-day-old autoclaved bio-ink mixture was mixed one last time with a handheld kitchen blender for 5 minutes until a homogeneous paste was obtained. This was done underneath a Bunsen burner and as sterile as possible. Of this bio-ink, 30 g was transferred to two 20 mL syringes with Luer screw locks. When printing with *C. reinhardtii* was desired, 2.10^7 cells of the stock prepared in section 2.1.1 were added to one of the syringes and thoroughly mixed with a long spatula, resulting in a light green mixture. If printing without algae was desired, the syringes could be used to print with bio-ink alone.

Before printing, the syringes were sealed with Luer plugs and centrifuged for 1 min at 3000 RPM to rid the syringes of bubbles. After centrifuging the syringes, the 3D printer was cleaned and the syringe was locked into the printer. When printing with gelatin, the syringe was heated to a maximum of 32 °C for about 15 minutes right before printing. This temperature limit is necessary as an abrupt transfer to a temperature above the typical growth range results in heat shock and cell death[39].

2.2 3D Printing

2.2.1 Printer Settings

3D printing was done with a customised Cura Ultimaker 2+. To accommodate the 20 mL syringe, a custom-built holder replaced the original filament extruder. Additionally, the Luer plug was replaced with a conical Luer dispensing tip with a nozzle opening of 0.84 mm. For optimal 3D prints with the desired volume and shape, the material flow was set to 125% of the original extrusion rate (0.5541 mm per 1 mm travelled), the feed rate was set to 1200 mm min^{-1} and the speed of the printer was selected to accommodate the smooth extrusion of the bio-ink filament. These specific percentages were visually selected through trial and error and yielded satisfactory results. To protect the microalgae inside the samples, the printing process took place inside a Petri dish, with the printer

bed remaining unheated throughout the process. The Petri dish was closed immediately after the print finished.

2.2.2 Crosslinking with $CaCl_2$

After extrusion, the samples were completely submerged for 5 minutes in $CaCl_2$ solution with a molarity of 0.2 M, unless stated otherwise. Here, ionic crosslinking happens, Na^+ ions dissociate from the alginate and the alginate polymer chains form new bonds with the double-charged Ca^{2+} ions. This crosslinking step increases the mechanical stability of the samples. After crosslinking, the Petri dishes were closed and stored in a box[12].

2.2.3 3D Printing Dimensions

For different testing objectives, several distinct 3D print dimensions and shapes were used. To test livingness and photosynthetic activity, samples were printed in cubes of 18x18x18 layers, resulting in a 14 mm edge, and for chlorophyll extraction, in cubes of 6x6x6 layers, resulting in a 4.7 mm edge. Examples of these samples can be found in Appendix B Figure B.3 and Figure B.1, respectively. The second printing shape, for rheology, was specifically designed to fit the plates of the rheometer. This shape was a disc with a thickness of three layers (2.3 mm) and a diameter of 20 mm (Appendix A Figure A.1). Lastly, profilometry samples, intended to analyze the sagging behaviour of the bio-ink, were printed in a similar shape as the paper by Kleger et al. (2019)[37] and the dimensions can be found in Figure A.2 Appendix A.2.

2.3 Parallel Plate Rheometry

Oscillatory measurements were performed using a HAAKE MARS III Rheometer equipped with serrated parallel plates (to minimize wall slippage) with a diameter of 20 mm. A constant gap distance of 0.75 mm was maintained throughout the experiments.

To determine the plateau moduli (G_0) of the samples, an amplitude sweep was conducted. The stress amplitude was increased logarithmically during the sweep, with selected strain rates (γ_0) ranging from 0.1% to 1000%, generating 60 data points. The experiments were carried out at a fixed frequency of 1 Hz. This specific range of strain rates was chosen as it proved sufficient for the bio-ink, effectively preventing slippage while providing the essential data. The entire process was conducted at room temperature and was closely monitored to avoid any undesired behaviour during the measurements.

2.4 Microscopy

In this research, several microscopy techniques were used to analyze the properties of the algae bio-ink, such as its sagging behaviour and livingness.

2.4.1 3D Laser Scanning Microscopy

The selection of an appropriate microscope to study the algae bio-ink's material structure and livingness on a micro-level started with exploring the suitability of 3D Laser Scanning Microscopy (3D-LSM). This was done with the KEYENCE VK-1000 series and imaging was conducted at various zoom levels, including 5x, 10x, and 20x. To perform this methodology, an algae cube was selected and the top face was subjected to imaging.

2.4.2 Confocal Laser Scanning Microscopy

Additionally, Confocal Laser Scanning Microscopy (CLSM) was employed to explore the use of chlorophyll autofluorescence properties inside the algae samples as a means to evaluate the livingness of the algae bio-ink. The CLSM equipment employed for this evaluation was the Nikon A1 Confocal Microscope, using the Nikon A1 Piezo Z Drive. The imaging was performed using two distinct excitation wavelengths: 405 nm and 488 nm. The third channel, the laser transmission, was used to generate a pseudo-widefield image. Each sample prepared for this method was cut in half. This was done to image the top face of the cube as well as the vertical square cross-section within the cube. The sample preparation is illustrated in Figure B.3 in Appendix B. The images were processed and analysed in ImageJ.

2.4.3 Optical Confocal Profilometry

To assess the sagging behaviour of the bio-ink, optical confocal profilometry was performed with the KEYENCE VR-5000. This technique allows for the measurement of the z-deflection of the spanning filaments as a function of the spanning distance. As mentioned in Section 2.2.3, the samples prepared for profilometry were printed in the dimensions for the overhang test.

2.5 Chlorophyll Extraction

The chlorophyll extraction protocol in Abu-Ghosh et al. (2021) was adapted for this research[40]. Here, the 3D-printed sample was placed in a 10 mL tube, followed by the addition of 2 mL of H_2O. The tube was then subjected to centrifugation at 4000 RPM for 10 minutes to separate the supernatant. The supernatant was carefully removed, and 1 mL of dimethyl sulfoxide (DMSO) was added under a flow cabinet. The sample was subjected to six cycles of freezing and thawing using liquid nitrogen. Subsequently, 2 mL of DMSO was added along with 2 glass beads with a diameter of 5 mm, and the mixture was vortexed for 5 minutes. After vortexing, the tube was centrifuged again for 5 minutes at 4000 RPM. The supernatant obtained from this step was used for measuring chlorophyll. Finally, the chlorophyll extract was pipetted into a 96-well plate, with 6 replicates for each sample.

2.6 Photosynthetic Activity Measurement Setups

To measure the photosynthetic activity of the samples, different experimental setups were built, each setup had three main sensors: a CO_2 sensor, a temperature sensor and a humidity sensor. All the different experimental setups can be found in Appendix C.1 through C.5.

The initial setup employed a 200 mL jar with a metal screw-on lid. This setup included sensors to measure the CO_2, temperature and humidity levels alongside the light status. The subsequent setup involved a 1 L glass bottle with a metal screw-on lid and white tape was wrapped around the lid for enhanced airtightness. An additional O_2 sensor was integrated into this setup. The third setup consisted of a 100 mL laboratory bottle with a blue plastic screw-on cap. From the third setup onward the O_2 sensor was omitted. All three initial setups involved creating a hole in the lid to accommodate the electric cables. To improve the airtightness the holes were sealed with epoxy glue.

In the pursuit of a completely airtight container, the final setup involved three 200 mL "weckpotten" or preserving jars. In this configuration, wireless sensors were implemented and the signals were transmitted from the sensors to the Raspberry Pi via infrared, while electricity was supplied using a wireless charging coil. Moreover, a light sensor was added, further automating the process. The fifth setup was finalised by adding separate fans around each jar to maintain a better temperature around the jar.

Chapter 3

Results

3.1 Mechanical Properties

In this section, the mechanical properties of the bio-ink are researched, which play a crucial role in determining its structural integrity and performance. Our study focuses on understanding the effects of various factors on the material's mechanical behaviour. Specifically, the influence of crosslink concentration, crosslink duration, algae growth, and the addition of gelatin on the material's mechanical properties are evaluated. To achieve this, a rheometer was used to conduct amplitude sweeps to get more information on the mechanical performance of the bio-ink.

Moreover, the sagging behaviour of the material was researched, as it is essential to understand how the material responds to gravity-induced deformation. To this end, profilometry was conducted to measure the z-deflection of the spanning filaments as a function of the spanning distance.

3.1.1 Effect of Crosslink Concentration

To investigate the impact of crosslink concentration, a series of experiments was conducted. Initially, fifteen discs were 3D printed without algae (Figure 3.1a), and an additional fifteen discs were printed with algae added to the bio-ink (Figure 3.1b).

The rheology samples were then submerged in various $CaCl_2$ concentrations, including 0.1 M, 0.3 M, 0.4 M and 0.5 M. Each concentration group consisted of three samples. Likewise, three non-crosslinked samples were included for a complete comparison. After printing and crosslinking, all samples were incubated for seven days before being subjected to an amplitude sweep with the rheometer. The figures[1] provided show the average results of the three samples for each concentration.

[1] In all figures the solid lines represent G' and the dotted lines represent G".

As shown in Figure 3.1, both graphs (a) and (b) demonstrate that the non-crosslinked and 0.1 M bio-inks have significantly lower storage ($G^{'}$) and loss ($G^{"}$) moduli compared to the other samples crosslinked with higher concentrations. The results indicate that the samples become tougher when treated with higher $CaCl_2$ concentration. Moreover, the algae bio-ink exhibits higher moduli in general compared to the bio-ink without added algae. For example, the algae bio-ink sample treated with 0.5 M $CaCl_2$ has plateau moduli of $G^{'}$ ($G^{'}_0$) and $G^{"}$ ($G^{"}_0$) at 2x10^5 Pa and 3x10^4 Pa, respectively, whereas the same sample without algae shows a $G^{'}_0$ just above 10^5 Pa and a $G^{"}_0$ of 2.5x10^4 Pa.

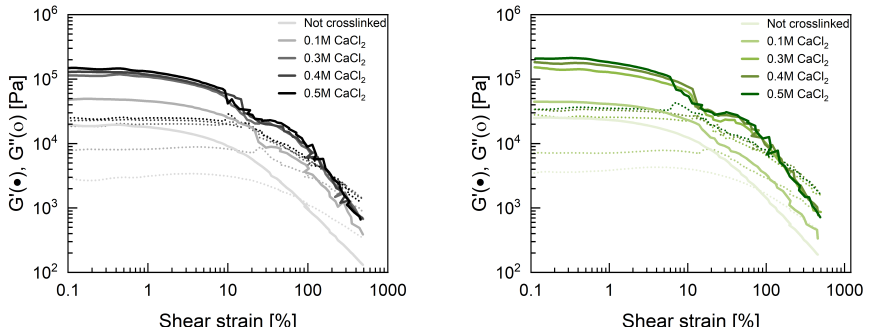

(a) Bio-ink without algae (b) Algae bio-ink

Figure 3.1: Oscillatory amplitude sweep of two times fifteen samples treated with $CaCl_2$ concentrations ranging from 0.0 M to 0.5 M, for 5 minutes. $G^{'}$ and $G^{"}$ [Pa] are plotted on the y-axis with a logarithmic scale and the shear strain [%] is plotted on the x-axis with a logarithmic scale.

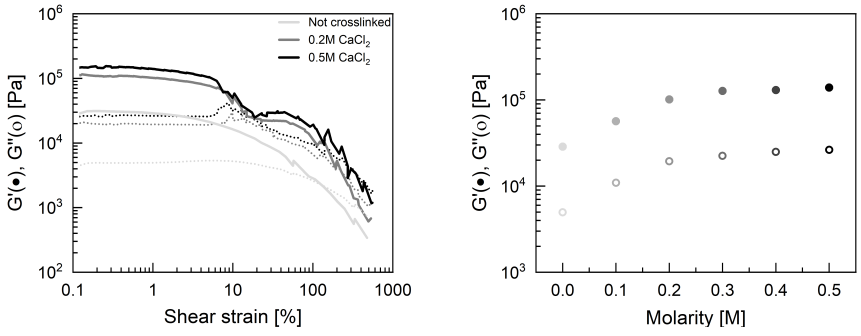

(a) Three selected concentrations (b) Complete pool

Figure 3.2: Oscillatory amplitude sweep of eighteen bio-ink samples treated with $CaCl_2$ concentrations ranging from 0.0 M to 0.5 M. (a) $G^{'}$ and $G^{"}$ [Pa] plotted against the shear strain [%] on logarithmic scales. (b) $G^{'}_0$ and $G^{"}_0$ plotted against crosslink concentration.

In Figure 3.2 another amplitude sweep was conducted on three samples for each of six $CaCl_2$ ranging from 0.0 M to 0.5 M (where 0.0 M is the non-crosslinked sample), resulting in eighteen samples without algae. Figure 3.2a illustrates the average results of the non-crosslinked samples together with the samples treated with 0.2 M and 0.5 M $CaCl_2$. Figure 3.2b shows the $G_0^{'}$ and $G_0^{"}$ values per $CaCl_2$ molarity.

In conclusion, the results from both Figure 3.1 and Figure 3.2 reveal a consistent positive correlation between the $G^{'}$ and $G^{"}$ moduli and $CaCl_2$ concentration, observed in both the bio-ink with and without algae.

3.1.2 Effect of Crosslink Duration

Continuing the research into the impact of crosslinking, the next subsection explores the influence of crosslink duration on the mechanical properties of the algae bio-ink. Figure 3.3 presents the average results of the oscillatory amplitude sweep of bio-ink samples without algae that were submerged in $CaCl_2$ with a molarity of 0.2 M for either 0, 5 or 60 minutes, per duration three samples were subjected to rheology.

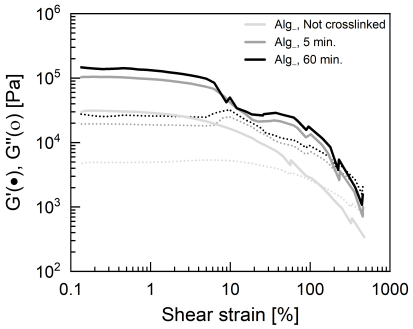

Figure 3.3: Oscillatory amplitude sweep curves of the average of three samples treated with $CaCl_2$ (0.2 M) for 5 minutes, the average of three samples treated for 60 minutes, and the average of three non-crosslinked samples. $G^{'}$ and $G^{"}$ [Pa] plotted against the shear strain [%] on logarithmic scales.

Here, it can be observed that crosslink duration impacts the rheology data. Particularly, there is a notable difference between the $G^{'}$ moduli of the non-crosslinked and crosslinked samples is significant. Additionally, there is a difference in the $G^{'}$ moduli between the 5-minute and 60-minute samples, although it appears to be statistically less significant.

3.1.3 Effect of Algae Growth

The following results depict the impact of algae growth on the rheology performance of the bio-ink. All samples were treated with 0.2 M $CaCl_2$ for 5 minutes.

In Figure 3.4, each curve represents the average of two samples.

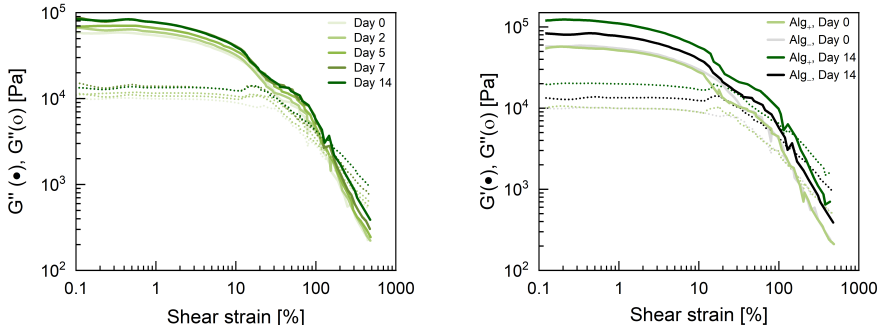

(a) (b)

Figure 3.4: Oscillatory amplitude sweep of samples treated with 0.2 M $CaCl_2$ for 5 minutes. $G^{'}$ and $G^{"}$ [Pa] are plotted logarithmically on the y-axis, and the shear strain [%] is plotted logarithmically on the x-axis. (a) Effect of algae growth for 0, 2, 5, 7 and 14-day-old samples. (b) Comparison of algae vs. no algae of 0 and 14-day-old samples.

In Figure 3.4a, the samples were incubated for different amounts of days, ranging from 0 days, where the sample was tested right after printing and crosslinking, to two weeks. The results show that there is a positive correlation between algae growth and the $G_0^{'}$ and $G_0^{"}$. In Figure 3.4b, control samples without algae were subjected to rheology to check if this correlation was indeed due to algae growth and not due to the drying of the samples. The results indicate that the moduli of the samples incubated for two weeks with and without algae lie above the samples tested right after printing. However, the samples with algae (Alg_+, Day 14) have a higher $G_0^{'}$ and $G_0^{"}$ than the samples without (Alg_-, Day 14), indicating that the samples with an algae growth of 14 days are tougher than the samples without algae growth.

In Figure 3.4a, the samples were incubated for various durations, ranging from 0 days (tested right after printing and crosslinking) to two weeks. The results demonstrate a positive correlation between algae growth and the $G_0^{'}$ and $G_0^{"}$.

To further investigate this correlation, Figure 3.4b includes control samples without algae, tested to determine whether the observed effects were due to algae growth or simply drying of the samples. The results reveal that the moduli of the samples incubated for two weeks, with and without algae, are higher than the samples tested right after printing. However, the samples with algae (Alg_+, Day 14) have higher $G_0^{'}$ and $G_0^{"}$ values compared to those without algae (Alg_-, Day 14), indicating that the samples with 14-day algae growth have a greater ability to store elastic energy and dissipate energy during deformation than the 14-day-old samples without algae growth.

3.1.4 Effect of Gelatin

The influence of gelatin on the mechanical properties of the algae bio-ink is investigated in this next experiment. All samples were treated with 0.2 M $CaCl_2$ for 5 minutes and then incubated for seven days. Figure 3.5 displays the results of the oscillatory amplitude sweep for four different sample types: algae bio-ink with gelatin, algae bio-ink, bio-ink with gelatin and the 'original' bio-ink.

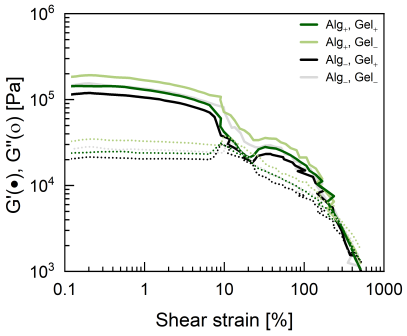

Figure 3.5: Oscillatory amplitude sweep four samples, with all combinations of algae and gelatin. All treated with $CaCl_2$ (0.2 M) for 5 minutes and incubated for seven days. $G^{'}$ and $G^{"}$ [Pa] plotted against the shear strain [%] on logarithmic scales.

Initially, it was anticipated that the addition of gelatin would enhance the mechanical properties of the bio-ink. However, the curve representing the sample with algae but without gelatin exhibits the highest values for $G^{'}_0$ and $G^{"}_0$. Surprisingly, the curve representing the sample with algae and with gelatin overlaps with the curve of the sample without algae and gelatin (just bio-ink), indicating that the addition of gelatin cancels out the benefits of the addition of algae growth. Furthermore, the curve representing the sample without algae but with gelatin added to the bio-ink exhibits the lowest values for $G^{'}_0$ and $G^{"}_0$ among the four samples. These unexpected results raise questions about the interaction between algae, gelatin, and the mechanical behaviour of the bio-ink.

3.1.5 Sagging Behaviour

The last mechanical test conducted on the bio-ink was to assess its sagging behaviour. This was done to evaluate the stability and structural integrity of the 3D-printed bio-ink. Figure 3.6 illustrates the results of this test.

The resulting 3D image provides insights into the material's behaviour during the test. However, it is worth noting that during imaging, scattering of the incoming laser occurred due to the components present in the bio-ink, which are all white powders before being solved in the Tris medium. As a result, the obtained image appears somewhat blurred and irregular.

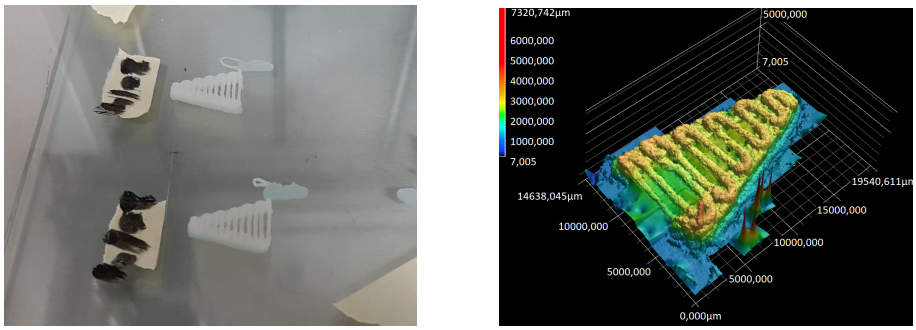

(a) (b)

Figure 3.6: Overhang test. (a) Some of the prints right after 3D printing. (b) 3D-topographical image obtained by profilometry, characterizing the filament bridging ability of the bio-ink.

Due to imaging challenges, the z-deflection of the spanning filaments as a function of the spanning distance could not be analysed properly. As one can observe with the naked eye, the spanning length of the longest bridge (the $10^t h$ bridge) was approximately 6.5 mm and was maintained by the bio-ink during the test. The z deflection of almost 2 mm of this bridge was significant, while the deflection of bridges one to four was quite tolerable. Despite the challenges of imaging, the test does provide a qualitative indication of the sagging behaviour of the bio-ink.

3.2 Livingness of the Algae Bio-Ink

This phase of the research delves into the exploration of a method to study the behaviour and growth dynamics of the algae cells within the bio-ink, aiming to unravel the intricate aspect of the livingness of this material. Investigating the living properties of the algae bio-ink has posed unique challenges throughout this study, presenting a fascinating yet complex chapter of the research.

To shed light on the livingness, several approaches were employed. First, the use of an inverted optical microscope was opted, to assess the possibility of examining the algae inside the bio-ink. However, the characteristics of the material hindered the imaging. Subsequently, the application of a 3D laser scanning microscope was explored, offering the potential to provide insights into the integration of the algae cells within the bio-ink structure. Yet again, the properties of the material only allowed for surface area imaging.

Following these attempts, the process of chlorophyll extraction was considered to quantitatively measure the presence of chlorophyll in the bio-ink. Regrettably, the bio-ink's complexity impeded the successful extraction of chlorophyll using this method. Finally, leveraging the auto-fluorescence of chlorophyll within the algae was pursued for fluorescence imaging with a confocal laser scanning microscope. Among the methods employed, this approach emerged as the most promising for studying the material's living properties.

3.2.1 First Results on Livingness and Micro Structure

To delve deeper into the livingness and structural characteristics of the material, a spectrum of imaging techniques was employed to examine the algae bio-ink. The exploration began with inverted optical microscopy, followed by 3D Laser Scanning Microscopy (3D-LSM).

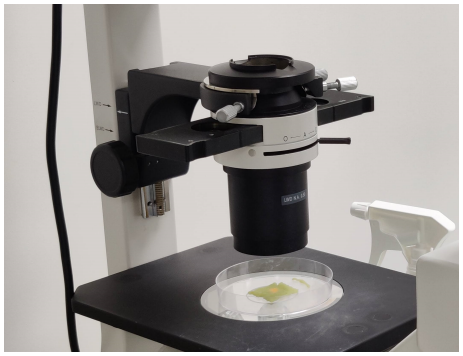

Figure 3.7: First Evaluation Using Inverted Optical Microscopy.

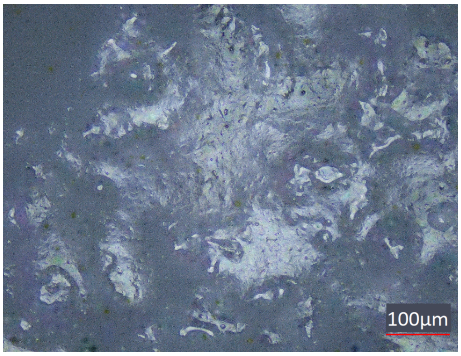

Figure 3.8: Result of the second evaluation using 3D-LSM.

Figure 3.7[2] presents the method of the first try to establish a method for quantifying cell count to get an indication of livingness within the 3D print. However, the use of the optical microscope for cell counting proved inadequate due to the material's opacity, preventing sufficient penetration of light for accurate cell counting.

As one can observe in Figure 3.8[3], the outcome of the 3D-LSM attempt shows a similar problem. Again, the material's opacity hindered the effectiveness of this technique as a suitable method to give more insight into the livingness of the algae samples. These results highlight the challenges associated with using these imaging techniques on the algae bio-ink.

3.2.2 Chlorophyll Content Evaluation

An additional approach to studying the livingness of the algae bio-ink over time that was explored involved the extraction of chlorophyll. In the initial trial, specially designed cubes with dimensions of 6x6x6 layers were 3D-printed to fit within 2 mL Eppendorf tubes. However, due to the smaller size of these cubes, maintaining the appropriate humidity level became challenging, resulting in the drying of the samples. Therefore, the original 3D-printing shape, a cube of 18x18x18 layers, was used for the chlorophyll extraction (Figure 3.9), following the protocol outlined in Subsection 2.5.

The first interesting observation in Figure 3.9a is the colour difference between the non-crosslinked sample and the crosslinked samples. After two weeks of

[2]Original image made by Vivian Vriend.
[3]See footnote 2.

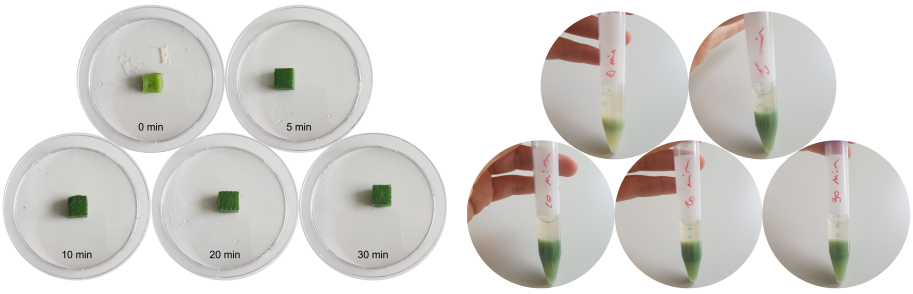

(a) (b)

Figure 3.9: The five samples and results of the chlorophyll extraction protocol. (a) The 3D printed cubes, all treated with 0.2 M $CaCl_2$, except for the 0 min sample, and incubated for 14 days before starting the chlorophyll extraction protocol. (b) The 10 mL tubes after the centrifugation step of the chlorophyll extraction.

incubation, the non-crosslinked sample is less green than the crosslinked ones. As the algae grow best in a humid environment, this phenomenon is attributed to the added moisture in the form of 0.2 M $CaCl_2$ when being subjected to crosslinking.

Unfortunately, the complexity of the bio-ink's composition rendered this method incompatible. Figure 3.9b illustrates the results of the post-centrifugation step. Contrary to expectations, the bio-ink and the algae chlorophyll remained intermixed after undergoing the chlorophyll extraction protocol. As a consequence of this outcome, it is evident that this method is not viable for the intended purpose and the supernatant could not be used to measure chlorophyll content.

3.2.3 Chlorophyll Auto-Fluorescence Evaluation

As depicted in Figure 3.10, the final technique employed to gain further insights into the livingness and structural characteristics of the samples involved the use of CLSM. This method enabled the capture of autofluorescence emitted from the chlorophyll present in the algae cells in the algae bio-ink samples. As illustrated in Appendix B Figure B.2, it was anticipated that the outer layer of the 7-day-old algae cubes would contain more living cells, and thus chlorophyll, than the inner layers of the algae cubes.

In Figure 3.10a, as expected, the upper layer of the 0-day-old algae bio-ink exhibits a relatively sparse density of algae cells. As an example, specific *C. reinhardtii* cells displaying the green autofluorescence of chlorophyll are highlighted with red arrows. Unfortunately, the signal-to-noise ratio of the image of the inside of the 0-day-old sample was too low and showed a completely green image (see Appendix B, Figure B.4). Similar anomalies were observed in the other laser channels, with Channel 1 displaying a completely blue image and

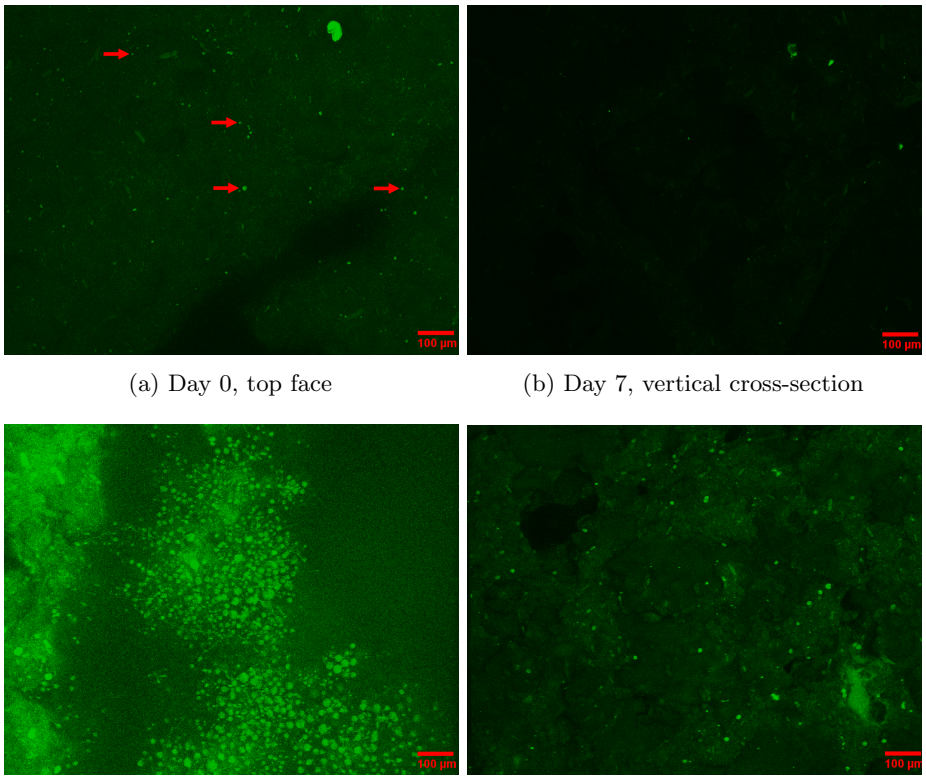

(a) Day 0, top face

(b) Day 7, vertical cross-section

(c) Day 7, top face

(d) Day 7, vertical cross-section

Figure 3.10: Top view of 3D stack CLSM images. All images were obtained with a laser wavelength of 488 nm in Channel 2, and all samples were treated with 0.2 M $CaCl_2$ for five minutes. (a) The top face of the cubical sample with algae, imaged on the day of printing. (b) The inner cross-section of the cubical sample without algae, imaged after a week of incubation. (c) The top face of the cubical sample with algae, imaged after a week of incubation. (d) The inner cross-section of the cubical sample with algae, imaged after a week of incubation.

Channel 3 rendering an entirely white image. Consequently, no direct comparison can be drawn with the inside of the 0-day-old algae bio-ink sample. Nevertheless, considering that the 18x18x18 layered cube is printed with a uniformly mixed algae bio-ink, it is reasonable to anticipate that the cell count in the inner part of the sample at day 0 should mirror that of Figure 3.10a.

Next to these first observations, the images of the 7-day-old samples all exhibit the expected cell count. In Figure 3.10b, no chlorophyll autofluorescence was observable due to the absence of added algae cells to the bio-ink. Whereas, the top surface of the 7-day-old cube printed with algae bio-ink features numerous *C. reinhardtii* cells. Figure 3.10d, shows a cell count similar to the cell count in the 0-day-old sample in Figure 3.10a.

The increase in cell count in Figure 3.10c can be allocated to the abundance of light penetrating the outermost layer of the cube. Whereas, the stagnation of cell count in Figure 3.10d can be allocated to the opaqueness of the bio-ink. To grow and multiply, algae cells need light and the composition of the bio-ink impedes the penetration of light to the centre of the cube.

In Figure 3.11 the integration of both Channel 2 and Channel 3 into a unified 3D image captures the upper surface of a 7-day-old algae bio-ink cube. As can be observed, the composition of the bio-ink is depicted in shades of grey, while the chlorophyll's autofluorescence is displayed in green. Notably, the MCC particles also emit a subtle green fluorescence, contributing to the overall green hue of the image.

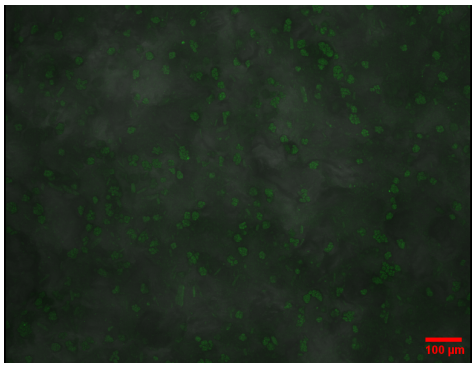

Figure 3.11: The top surface of a 7-day-old algae bio-ink cube where both Channel 2 and 3 were merged into one image. The sample was treated with 0.2 M $CaCl_2$ for five minutes.

In conclusion, studying the livingness of this complex and opaque bio-ink presents substantial challenges. After numerous attempts, CLSM emerged as the best technique thus far, leveraging the autofluorescence of chlorophyll within the algae cells and MCC within the bio-ink to provide further insights into the livingness of the 3D-printed samples as well as giving some indication of structural composition.

3.3 CO_2 Release of 3D Printed Bio-Ink

This section delves into the outcomes obtained from the experimental setups designed to assess the photosynthetic activity of the algae bio-ink samples. The first setup focused on monitoring CO_2, temperature, and humidity levels of a 3D-printed algae cube over time. Then a second test was conducted where O_2 was measured as well. Following these findings, a subsequent investigation was conducted to evaluate how varying the medium type of the sample – TAP, Tris, or H_2O – influenced the release of CO_2 levels by the bio-ink. Additionally, the influence of treating Microcrystalline Cellulose (MCC) on the CO_2 release of the bio-ink was measured over time.

3.3.1 Photosynthetic Activity Testing

During this research project, multiple iterations were gone through, from studying the photosynthetic activity of the living material to measuring the CO_2 release of the non-living bio-ink. All setups are detailed in Chapter 2 and illustrated in Appendix C.1 through Appendix C.5. Additional results can also be found in these sections in Appendix C.

First Setup

The outputs[4] from the first measuring setup are depicted in Figures 3.12 and 3.13. A control was performed by measuring the levels in an empty box, these results are illustrated in Appendix C.1 Figure C.2.

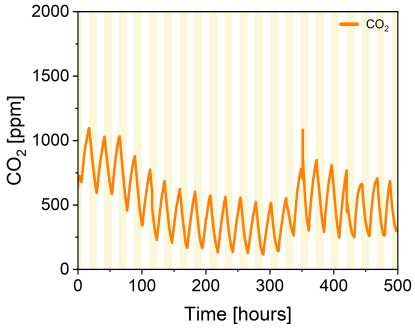

(a) CO_2 level of algae bio-ink

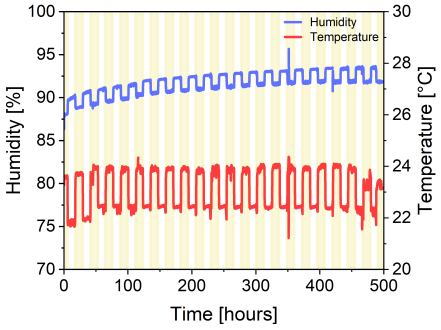

(b) Hum. and temp. of algae bio-ink

Figure 3.12: CO_2 (3.12a), humidity (3.12b), and temperature (3.12b) levels inside Setup 1 containing a 3D printed 18x18x18 layered sample with algae (2.2 g), measured over three weeks.

Figure 3.12a illustrates the photosynthetic activity of the algae bio-ink. As expected, the CO_2 level shows a decrease during the light phase and an increase during the dark phase. Furthermore, a gradual reduction in the relative CO_2 level over time could indicate the proliferation of algae within the sample, actively capturing carbon dioxide from the surrounding air. The CO_2 increase around the 350^{th} hour coincided with opening the bottle, which similarly caused a peak and a dip in humidity and temperature, respectively.

Figure 3.12b demonstrates the predictable pattern of the temperature rise from 22 °C to 24 °C during light exposure, leading to a reduction in relative humidity from approximately 93% to 92% due to the elevated temperature.

[4]In all the sensory output figures, the yellow area in the figures indicates when the light was turned on in cycles of 12 hours.

The second output is shown in Figure 3.13, and in Figure 3.13a, two peaks in the measured CO_2 level independent of light exposure can be observed. As no such trend was observed in Figure 3.12a, the peaks in Figure 3.13a suggest that the material releases CO_2 when no algae are added to the bio-ink. Moreover, there is a rapid decline in the CO_2 level which could be attributed to a jar leak. In Figure 3.13b, the temperature again fluctuates from 22 °C to 24 °C and the relative humidity fluctuates steadily around 91%.

If the jar was indeed leaking, the decrease in the reading of Figure 3.12a might also be due to leakage instead of carbon capturing, rendering the results inconclusive. Moreover, the temperature and humidity in the control (Figure C.2b) did not follow the characteristic fluctuations seen in the other experiments and it was decided to design a new setup. The reason for the second peak in Figure 3.13a remains unknown.

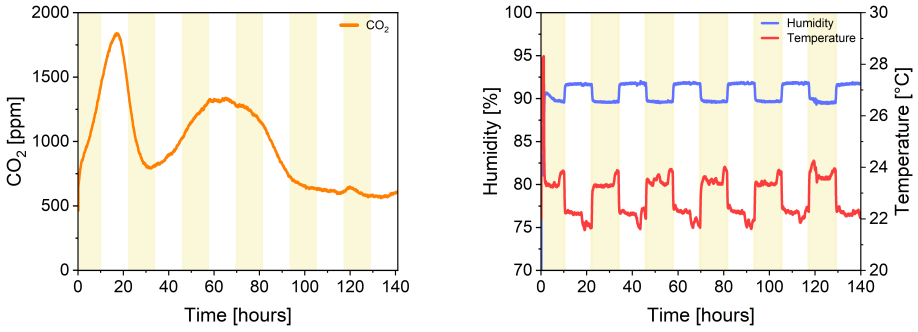

(a) CO_2 level of bio-ink (b) Hum. and temp. of bio-ink

Figure 3.13: Measurements inside Setup 1 containing a 3D printed 18x18x18 layered bio-ink sample without algae (2.2 g), measured over six days.

Second Setup

As previously mentioned, the second setup also incorporated an O_2 sensor. The resulting measurements are presented in Figures 3.14a and 3.14b. The humidity measurement can be found in Appendix C.2 Figure C.4.

The measurements depicted in Figure 3.14a reveal that the O_2 level increases as anticipated when the light is on, and simultaneously, the CO_2 level decreases. However, upon examining Figure 3.14b depicting the O_2 graph and the temperature graph, a notable alignment between the O_2 and temperature readings becomes evident. The algae bio-ink's release and uptake of O_2 is too small in relation to the 21% atmospheric oxygen that the measuring of O_2 rather relates to the temperature level, or in other words the relative oxygen content increases when the temperature increases and this is measured by the sensor. Additionally, the CO_2 level exhibits fluctuations around 500 ppm, displaying a slight upward trend. This subtle trend might have originated from the CO_2 release of the bio-ink, potentially diminished by leakage.

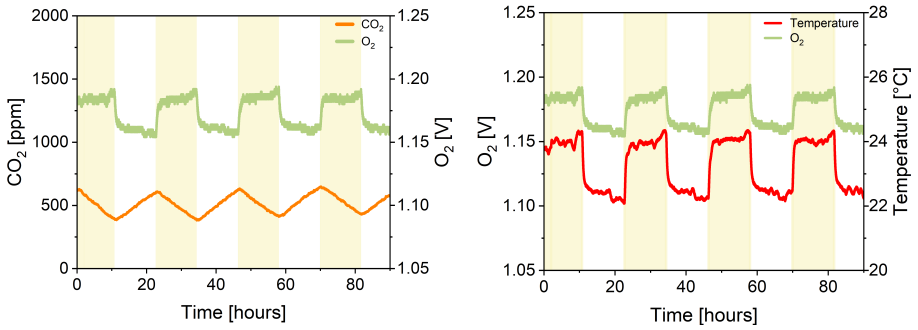

(a) CO_2 and O_2 of algae bio-ink (b) O_2 and temperature of algae bio-ink

Figure 3.14: Output of the measurements inside Setup 2 containing a 3D printed 18x18x18 layered bio-ink sample with algae (2.2 g), measured over four days.

To understand the origin of the CO_2 peak observed in Figure 3.13a, indicating a release of CO_2 from the bio-ink, the focus of the study transitioned from investigating the photosynthetic activity of the algae bio-ink to an exploration of the underlying causes of this CO_2 release phenomenon.

3.3.2 Shift to Studying CO_2 Release

Third Setup

Additionally, a third setup, illustrated in Appendix C.3 Figure C.5, was designed with enhanced airtightness in mind. Below, in Figure 3.15 the CO_2 measurements and in Appendix C.3 Figure C.6 the humidity and temperature measurements of the first two experiments are depicted.

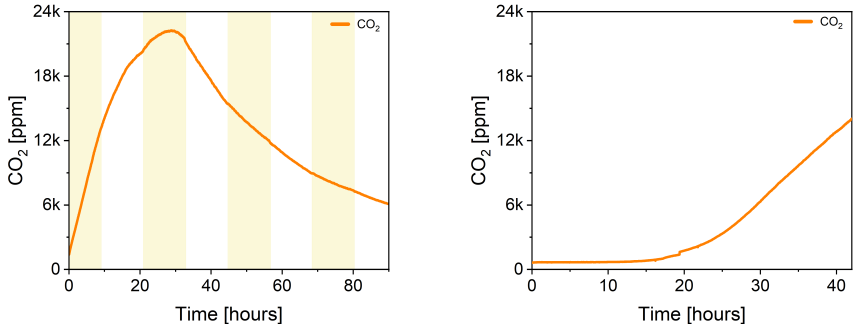

(a) (b)

Figure 3.15: CO_2 release of (a) the bio-ink without algae, measured over 4 days, and (b) the non-autoclaved Tris and MCC mixture, measured over 42 hours.

As one can observe in Figure 3.15a, the original bio-ink without algae again releases a great amount of CO_2 right at the start of the measurement. At a level of 22.500 ppm, around the 30^{th} hour, the CO_2 level decreases. In Figure 3.15b, the release of CO_2 of the Tris-MCC mixture starts around the 20^{th} hour and increases to approximately 15.000 ppm when the measurement was stopped.

After these experiments, a control measurement was done on a small amount of water and showed an insignificant increase in CO_2. Then a measurement was conducted on an autoclaved Tris-MCC mixture. The results of these two experiments can be found in Appendix C.3 in Figures C.7 and C.8.

The redo of the fourth experiment, and the last experiment done in this setup, can be seen in Figure 3.16.

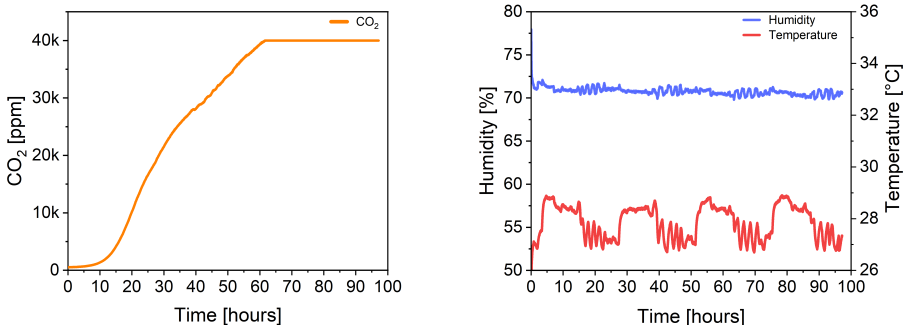

(a) (b)

Figure 3.16: Second try of the CO_2 release measurement of the autoclaved Tris and MCC mixture, measured over 100 hours.

Again, an autoclaved Tris-MCC mixture was inserted in the jar and measurements were collected for almost 100 hours. The temperature and humidity readings fluctuated around 27.5 °C and 71%, respectively. The relative humidity fluctuates a bit less than the previous readings, this could be attributed to the change of setup.

The CO_2 release of the autoclaved Tris-MCC mixture started around the 10^{th} hour, so 10 hours prior to the non-autoclaved Tris-MCC mixture in Figure 3.15b. Here, the peak increased a considerable amount and around the 60^{th} hour the sensor was saturated by the CO_2 release of the sample. This result indicates that autoclaving the Tris-MCC mixture does not mitigate the CO_2 release.

3.3.3 Media Test: Tris, TAP or H_2O

Fourth Setup

The next step was to investigate the effect of switching the bio-ink preparation medium from Tris to Tris Acetate Phosphate (TAP) or demineralized water. This experiment was designed to determine whether MCC with different media produced a larger or lower peak in CO_2 release. Because TAP has a higher carbon content than Tris, it was expected that the CO_2 peak from this medium would lie higher. The release from the H_2O mixture, on the other hand, was expected to be lower. The new setup consisted of three preserving jars that could measure simultaneously.

To carry out this experiment, samples were prepared by combining the MCC with one of the three media as described in Subsection 2.1.2, mixing for 5 minutes, and then allowing it to sit on the bench for 15 minutes. After another thorough mixing, the different MCC-medium combinations were autoclaved. After two days in the 30 °C room, they transferred to three caps from a plastic tube and put into the fourth setup, illustrated in Appendix C.4 Figure C.9[5].

As one can observe in Appendix C.4 Figure C.10, the CO_2 graphs of the first try begin rather high. In other words, the reading began after the samples had been in the jars for quite some time. Furthermore, the caps used in this first iteration were quite large, originating from 50 mL tubes and each containing 5 g of the mixtures. As a result, there was a lot of condensation inside the jars.

To avoid condensation, a second attempt with smaller caps was made, as shown in Figure 3.17.

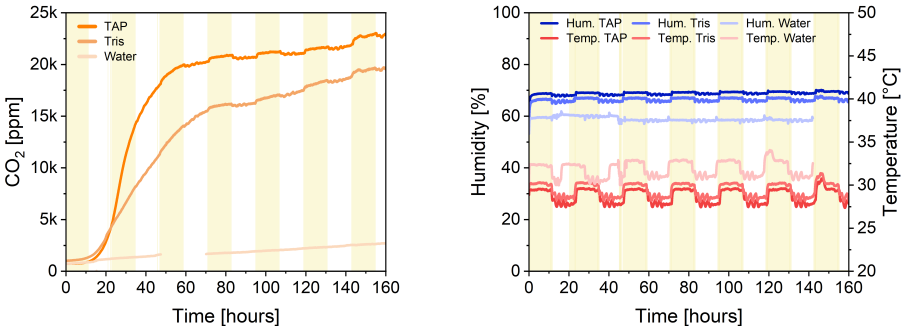

(a) (b)

Figure 3.17: Measurements over 160 hours of MCC with H2O, Tris or TAP as a media. All samples were autoclaved and weighed 3.25 g.

The first observation is that the mixture including TAP has the greatest increase in CO_2 level, whereas the mixture containing water has the least increase. As a result, it can be hypothesized that the excessive CO_2 release originates

[5]The samples were not printed, making the experiments less time-consuming.

from combinations containing MCC and a carbon-containing media. Tris has a lower carbon content than TAP, hence the overall CO_2 level remains lower.

Furthermore, the TAP and Tris temperature readings now range from 27 °C to 32 °C, whereas the water temperature reading even ranges from 30 °C to 32.5 °C. This is most likely due to the additional electronics inside the fourth setup, which causes a higher overall temperature inside the large box.

Lastly, in the CO_2 graph of the water sample, the sensor transmitted several faulty readings, resulting in an incomprehensible sensory output. In Figure 3.17a, these outputs were masked. In Figure 3.17b, they resulted in a 20-hour shift to the left in both the humidity and temperature graphs of this sample.

Overall, the results of these experiments demonstrate that medium has an effect on CO_2 release when mixed with MCC. TAP mixed with MCC has the most CO_2 release, whereas water has the lowest CO_2 release.

3.3.4 MCC Test: MCC, MCC_+ or MCC_t

In addition to the media test, an attempt was made to treat the MCC before it was added to Tris and used to make the bio-ink. The first approach involved baking 3.6 g of MCC powder for 1 hour at 100 °C without a lid. This MCC will be called MCC^+. The second method was to treat 3.6 g of MCC with Hydrazine Monohydrate and is depicted in Figure C.12 Appendix C.5.

In the first experiment, three samples were made: a Tris-MCC mixture and a Tris-MCC^+ mixture, both made as described in the previous section and a bio-ink sample where MCC^+ replaced the MCC. After autoclaving both mixtures and the bio-ink, 3.55 g of each sample was placed in a cap of a 10 mL plastic tube. Unfortunately, these samples were prepared during the fungal contamination period (also referred to as "FungiGate"), and all earlier setups (including the fourth setup), current samples, and so on had to be discarded to prevent further contamination. Therefore, no measurements were done on these samples.

Fifth Setup

The fifth setup consisted of three new preserving jars with wireless CO_2, humidity and temperature sensors in each jar. In this setup, the large box was replaced with smaller 3D-printed "cages" for each of the jars individually. Figure C.11 in the Appendix depicts this setup.

Three separate samples were prepared for the second experiment. For the first sample, the original bio-ink was used. The MCC was substituted by MCC^+ and MCC_t in the second and third samples, respectively. Figure 3.18 depicts the powders for 100 mL of each bio-ink. All bio-inks were autoclaved and 2.6 g of each bio-ink was placed in a cap (10 mL in one of the jars.

As one can observe in Figure 3.18 below, the MCC_t was burned in the process of being treated with Hydrazine Monohydrate.

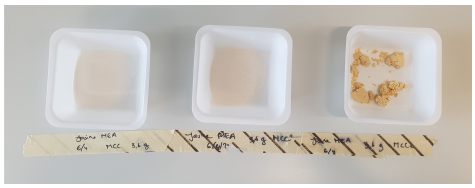

Figure 3.18: The three MCC types used in the samples, before being mixed into the bio-inks.

The measurements of this experiment are depicted in Figure 3.19. Unfortunately, the lamp's time switch was not turned on, leaving the samples in the light phase for the duration of the experiment. Furthermore, no excessive CO_2 release is seen in the original bio-ink sample, while this was seen before in Figures 3.13a and 3.15a. Similarly, the MCC$^+$ bio-ink increases by less than 25 ppm. Only the MCC$_t$ sample shows an increase. However, this increase of 250 ppm is still insignificant when compared to the increase of 1.000 ppm in the first setup containing an original bio-ink sample of 2.2 g (Figure 3.13a).

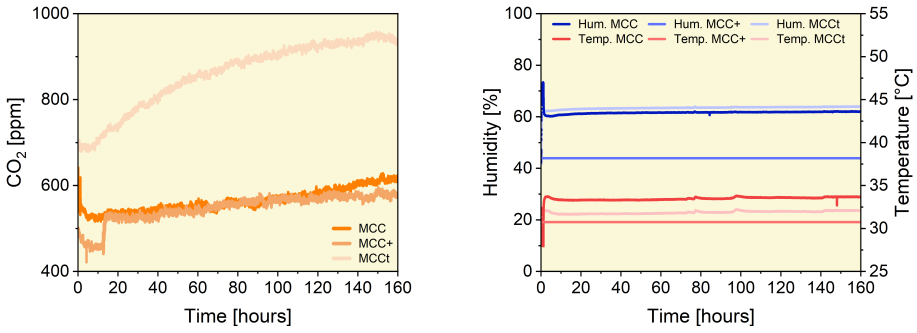

(a) (b)

Figure 3.19: Measurements over 160 hours of MCC, MCC$^+$ and MCC$_t$ bio-ink samples. All samples weighed 2.6 g.

The temperature and humidity graphs in Figure 3.19b lack the distinctive fluctuations seen in previous figures. Given that the light was never turned off, this was not very surprising. Furthermore, the highest temperature in this setup is slightly higher than desired (MCC: 34 °C), resulting in a relative humidity level of just 60% (MCC and MCC$_t$) and 40% (MCC$^+$). As this high temperature can be detrimental to the algae in the bio-ink[39] and low relative humidity causes drying of the hydrogel-based ink, this should be circumvented in future experiments.

The results of this experiment are quite counteractive and contradicting because of the lacking peak in CO_2 release in the original bio-ink sample. Therefore, this result cannot be compared to previous measurements. Also, the

MCC_t was burned in the treating process, raising questions about the reliability of the CO_2 reading.

Due to the inconclusive nature of this result, leakage tests were done. The first results show that the jars were indeed not airtight and jars 1 and 2 leaked a considerable amount of CO_2. Before a second leakage test was conducted the rubbers of the jars were replaced. The results show that the jars are now airtight and hold a considerable amount of CO_2. However, the leakage test only lasted for 2.5 hours, decreasing the reliability of the test. The results of these tests are included in Figures C.13 and C.15 in Appendix C.5.

3.3.5 Bio-ink Age Test

In this experiment, fans were added to each one of the "cages" of setup five, this was done to decrease the temperature by providing better airflow around the jars. The bio-inks for this experiment were made on different days before being placed into the jars. The original bio-ink ages were 21, 7 or 0 days old. Expected was that as the original bio-ink aged, the ink would release less CO_2. Unfortunately, this was not observed in the results shown in Figure 3.20.

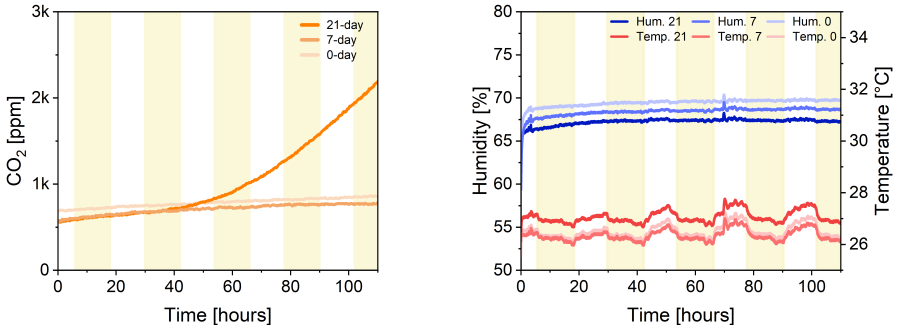

(a) (b)

Figure 3.20: Measurements over five days of 21, 7 or 0-day-old bio-ink. All samples were autoclaved and weighed 2.3 g.

The 21-day-old sample was the only sample that exhibited a rise in CO_2 level and the CO_2 release started 30 hours later than previous measurements. It is uncertain why the increase in CO_2 started around the 50^{th} hour and why the other samples did not show any increase at all adds to the oddity of this experiment. The jars were tested for leaks, and as previously stated, the jars should be airtight, thus it is improbable leakage is the problem. On a positive note, the temperature remained stable around 26.5 °C with the introduction of fans, offering promise for future experiments. Due to the extensive research conducted thus far and the unfortunate time constraint of a Master End Project, this experiment marks the conclusion of the research project.

Chapter 4

Discussion

4.1 Mechanical Properties of the Living Material

4.1.1 Crosslinking Increases Sample Stability

Crosslinked samples demonstrated improved stability compared to their non-crosslinked counterparts when subjected to rheology. The difference between the G' moduli of non-crosslinked and crosslinked samples was significant, whereas the difference between the 5-minute and 60-minute samples appears to be insignificant. Furthermore, it's noteworthy that crosslink concentration appears to be a pivotal factor, impacting not only the toughness of the material but also the growth of algae as was seen in Figure 3.9a. Based on the data presented in Figures 3.1 through 3.3 in Chapter 3, the sweet spot for molarity of $CaCl_2$ seems to be in the range of 0.2 M to 0.3 M and for the crosslinking duration it seems 5 minutes results in a favourable toughness.

4.1.2 Algae Growth Increases Sample Stability

The favourable effect of algae development on the toughness of the material emphasizes the relevance of the living material. Toughness increases when algae grow within the material. However, it is crucial to note that this process takes time, at least two weeks and an alternative explanation for the increased toughness could be the gradual drying of the sample due to evaporation. If that is the case, the algae do not provide structural hardening over time. Still, the algae seem to grow and the material becomes tougher over time, which is a desired outcome of these experiments.

4.1.3 No Benefits of Adding Gelatin

Contrary to crosslinking and algae growth, the addition of gelatin does not yield favourable results concerning the material's mechanical properties. Not only does it fail to improve the material's characteristics, but it also presents

practical challenges in handling within the laboratory environment as it needs to be liquified by increasing the temperature. This, in turn, can be detrimental to the algae, as is illustrated in the figures provided in Appendix A Figure A.1.

4.1.4 Sagging Behaviour of the Bio-Ink

The overhang test done with the bio-ink, resulting in a maximal spanning length of 6.5 mm, showed the promising properties of the material, similar to the results in the paper by Kleger et al. (2019) [37]. However, it is good to consider the rapid drying of the hydrogel-based material, which can introduce variability and complexities into these measurements. Moreover, the scattering of the material poses further challenges, hindering the acquisition of precise topographical images and the accurate analysis of z-deflection with respect to spanning length. Potential avenues for future research include exploring methods to reduce scattering (Figure A.3) properties, such as employing a high-speed mixer for a smoother texture or considering the use of colouring agents to mitigate scattering effects.

4.2 Analysis of the Livingness of the ELM

Cell counting under an optical microscope presented substantial challenges due to the opaqueness of the bio-ink. The complex composition of the material rendered it virtually impossible to conduct accurate cell counts using traditional microscopy techniques. Attempts to separate chlorophyll from the bio-ink for the quantitative study were met with similar setbacks. The hydrogel-based material's complicated composition proved to be a severe obstacle to isolating chlorophyll from the surrounding matrix. These limitations in chlorophyll extraction and optical imaging highlight the difficulties in analysing the material's livingness.

The last technique, imaging the living material with CLSM by exploiting the chlorophyll autofluorescence of the algae, revealed some initial valuable insights into the ELM's livingness and structural composition. The use of two distinct excitation wavelengths of 405 nm and 488 nm in Channels 1 and 2, obtained clear and high-resolution images as shown in Figure 3.10. And as expected, the inside of the 7-day-old algae cube contained less chlorophyll than the top layer of the algae cubes. Nonetheless, some anomalies were encountered, as shown in Appendix B.3. Due to the limited penetration depth of confocal microscopes the living material had to be cut in half, resulting in one-time imaging of thick samples. Additionally, high-resolution images require significant acquisition times. Nonetheless, imaging the ELM using CLSM proved the most promising technique for future investigation, thus far. It offers a potentially fruitful direction for future studies in the analysis of the structure and livingness of this living material.

4.3 Photosynthetic Activity Analysis

4.3.1 CO_2 Release of the Non-Living Material

The results of the photosynthetic activity analysis present a complex picture. One of the notable results is the increase in CO_2 levels at the beginning of the measurements of bio-ink and Tris-MCC mixtures without algae.

This phenomenon sparks several questions regarding the underlying mechanisms. Could the oxidation of the bio-ink to CO_2 by oxidants, originating from either the microcrystalline cellulose or sodium carboxymethylcellulose in the MCC mix, be the contributing factor to this initial rise in CO_2 levels[41;42;43]? This question raises another: does this increase in CO_2 offset the benefits of photosynthetic activity? While it is evident that the CO_2 can be utilized by the algae, the significant peak observed during the experiments raises concerns. Is this peak too high for the bio-ink to have any meaningful positive effect on climate change?

It would be worth exploring why MCC seems to play a role in this rise in CO_2 levels, especially in further comparison to experiments with H_2O or TAP. Additionally, it might be interesting to redo the experiments with MCC_t and MCC^+ on this reaction. Lastly, in this research project, the peak was not seen in the first results where the bio-ink contained algae. Therefore, it would be very interesting to study if this peak will present itself in similar conditions and in the presence of algae in the bio-ink.

Understanding these dynamics can shed light on whether this CO_2 peak could be mitigated to decrease the carbon footprint of the material and make sure that the algae use the atmospheric CO_2, as that is the ultimate goal of this ELM.

4.3.2 No CO_2 Release in the Final Experiments

The last results from Section 3.3.4, where the effect of using different types of MCC was tested, and Section 3.3.5, which entailed researching the impact of the age of the bio-ink, on the CO_2 release, raise questions. Due to the frequent occurrence of CO_2 release, in humidity conditions ranging from 90% to 70% and temperature conditions from 22 °C to 30 °C, the lack of a peak in these results was unexpected. However, when looking at the breath test following this experiment (Figure C.13 Appendix C.5), the lack of CO_2 release in Figure 3.19a can be attributed to leaks in jars 1 and 2, which were the containers for MCC and MCC^+, respectively.

However, the results in Figure 3.20a were obtained after the second leakage test (Figure C.15 Appendix C.5) and lacked a rise in CO_2 in the 0 and 7-day-old samples. Here, the lack of a peak could be linked to a lower level of relative humidity. In this bio-ink age test the temperatures (26 °C - 27 °C) lie in the previously measured temperature range (22 °C - 30 °C) where peaks were observed, however, the relative humidity lies around 67%, 3% lower than the other measurements where peaks occurred. This small change in humidity could

be the reason why the release of CO_2 did not occur in these samples. However, airtightness could still play a role in the lack of rising CO_2 levels.

4.3.3 Setup Challenges

The most important challenge has been hinted at several times: the airtightness of the measurement setup. Several practical challenges, including the drying of rubbers and metal fatigue of the lids, were encountered with the preserving jars used in the fourth and fifth setups affecting at least the MCC test and maybe also the bio-ink age test. Leakage also emerged in the other setups, affecting the accuracy of the data gathered with the first four setups.

Another significant challenge throughout this study was the variation in experimental setups. With the setup changing five times in total, drawing definitive conclusions becomes challenging. Each iteration of the setup brought its own set of complications, from an increase in temperature to humidity issues.

Furthermore, the measurement of O_2 was completely left out as the increase in these levels was too little to measure correctly. Issues such as the drying out of rubber seals on the preserving jars and the buildup of condensation inside the jars further complicated these experimental setups.

4.3.4 Effect of Seasonal Variations

Furthermore, seasonal variations in humidity and temperature were observed during the different experimental setups. Setups 1 and 2, conducted in the summer, experienced higher relative humidity. In contrast, setups 3, 4, and 5, carried out in winter and spring, faced lower humidity levels. These variations could impact the outcomes and need to be considered in the interpretation of results.

Overall, these complex factors influenced the measurements of the experimental setups. It underscores the importance of addressing practical challenges to ensure the reliability of the data and emphasizes the need for a comprehensive understanding of the variables at play in future research.

4.4 Challenges in the Production Process

4.4.1 Living Material Behaviour

The production process of the living material revealed several significant challenges. One of the primary concerns was the material's inherent tendency to undergo rapid shrinkage. This presents practical difficulties as it is challenging to maintain the desired structural integrity. This means that finding suitable applications for the material will prove difficult. Moreover, the algae grow best under strict climate control, including lighting conditions. While essential for promoting algae growth, the required control of environmental climate to promote algae survival may pose challenges in possible applications. The seasonal impact on humidity further complicates matters, in summer the material will dry

out even faster and this will cause shrinkage and algae cell death as the water in the sample evaporates. Unpredictable dying of the algae at times introduced additional complexities into the research process.

Another challenging factor of working with living materials is that the disposal of living cells has to be done according to strict policies. To adhere to regulations, the material must first be killed using ethanol or discarded in a designated bin. In order to make applications in industrial or commercial contexts feasible, this challenge needs to be addressed.

4.4.2 3D Printing Challenges

While 3D printing offers the advantage of creating complex and customizable shapes, the 3D printing process in itself posed its own set of difficulties. Continuous supervision during printing was necessary, primarily because the samples were relatively small, requiring immediate initiation of new prints upon completion. Moreover, the environmental conditions in the aerospace engineering workspace where the printing occurred were not ideal, raising concerns about potential contamination. The shared use of the printer for various organisms and materials heightened the risk of unintended cross-contamination.

Another noteworthy challenge was the inconsistent behaviour of the ink during the 3D printing process. Each print job exhibited variations, necessitating several iterations before landing on a suitable protocol. It is possible that these inconsistencies were related to the protocol used for ink preparation, especially since the mixing was done with a hand-held mixer. Additionally, printing within Petri dishes introduced some minor complications, especially when the placement of the dish was not precise.

4.4.3 Contamination During Ink Preparation

Issues related to ink preparation and handling before printing also surfaced as significant challenges. Contamination concerns arose as the process sometimes resulted in contamination even before the printing began. For instance, as seen in Figure D.2 in Appendix D, a 3-week-old ink stored in a beaker covered with aluminium foil exhibited a yellow growth after being kept in the 30 °C room for three weeks.

4.4.4 Laboratory Environment

As mentioned a few times before, a clean laboratory environment plays an important role in the overall success of a research project. A clean workspace is essential to prevent contamination and ensure the reliability of experiments and prints. The open design of the Cura Ultimaker 2+ printer presented an increased risk of contamination, as it easily allows foreign particles or organisms to enter the 3D printer during the printing process. Additionally, the bio-ink used in the research is a perfect breeding ground for the growth of other organisms,

including fungi. This complicates the process of designing suitable experimental setups, such as the CO_2 measuring setups.

4.5 Sustainability Within Academia

Throughout the course of this research project, another important challenging aspect was observed: sustainability in the research environment. Despite doing research in sustainable carbon-capturing materials, a considerable amount of plastic was used and discarded during the research process. This included disposable plasticware (e.g. gloves, pipet tips, Petri dishes) and supplies that, while important for experimentation, contribute to plastic waste. Furthermore, the use of equipment that consumes a lot of energy, such as autoclaves and many other electrical devices used during this research, has a substantial carbon footprint[44]. This observation highlights an important point: academic research, even when aimed towards sustainability, can have a significant environmental impact.

In light of these findings, it is critical that academia create and design more sustainable research practices, including the development of environmentally friendly laboratory protocols, materials, and equipment. By reducing the reliance on single-use plastics and minimizing energy consumption in research, academia can align its actions more closely with the principles of sustainability that underpin much of its work. Because academia plays a central role in addressing global challenges like climate change, incorporating sustainable practices within its own process will not only contribute to a more ecologically responsible academic community and set a positive example but will also support the message sent while doing this sustainability research.

Chapter 5

Conclusions and Recommendations

5.1 Conclusions

As part of the global effort to promote sustainability and combat climate change, this research on a biodegradable photosynthetic living material makes a positive contribution to these goals. During this project, the mechanical properties, livingness and photosynthetic activity of a hydrogel-based living material containing *C. reinhardtii* were researched. This research project builds upon earlier research done by Balasubramanian et al.[34] and uses the material developed in the master thesis of Vivian Vriend[12].

The results of the rheology tests conducted in this research showed that treatment with $CaCl_2$ improves the mechanical properties of the bio-ink, with and without algae, compared to the non-crosslinked samples. Furthermore, the duration of crosslinking shows a significant difference between the G' moduli of non-crosslinked and crosslinked samples, whereas the difference between the 5-minute and 60-minute samples appears to be far less significant. Moreover, it was observed that crosslink concentration appears to be positively correlated with the toughness of the material and also stimulates the growth of algae.

The sweet spot for molarity of $CaCl_2$ seems to be in the range of 0.2 M to 0.3 M and for the crosslinking duration it seems 5 to 10 minutes results in a favourable toughness. Next to this, algae growth was also found to have a positive impact on the toughness of the bio-ink. During all these experiments, it should be taken into account that samples dry over time and this might affect the hardness of the samples, affecting the rheology measurement.

The best-performing algae bio-ink sample had plateau moduli of $G"(G_0') \approx 2\text{x}10^5$ Pa, and $G" (G_0") \approx 3\text{x}10^4$ Pa. In practical terms, these values correspond to a toughness where the cubes are strong enough to retain their shape, but they can still be squished and destroyed by pinching them hard with your fingers. As such, the material strength of the bio-ink is currently too low to use in any structural applications.

The initial results of the photosynthetic activity measurement, aimed at assessing the carbon-capturing potential of the algae bio-ink, appeared promising. The CO_2 measurements behaved as expected. These oscillated based on the lights being on or off and showed an overall downward trend which indicated that the algae were successfully capturing carbon over time. Unfortunately, issues with the test setup mean these results were inconclusive. Jar leakage, for example, could not be ruled out as a cause of the downward CO_2 trend. This was addressed in later test setup iterations. Moreover, unexpected peaks in CO_2 readings were observed. As such, the research shifted its focus towards a thorough investigation of the underlying factors contributing to the significant CO_2 release from the bio-ink without algae. During the tests that followed, the TAP-MCC mixture showed a release of CO_2 of 22.500 ppm and the Tris-MCC mixture of almost 20.000 ppm. Treatment of MCC by baking it in an oven at 100 °C and curing it with Hydrazine Monohydrate gave inconclusive results as the airtightness of the setups proved insufficient. Trying to figure out the impact of the age of the bio-ink on the CO_2 release resulted in unexpected readings and the reason behind these results remains unknown. Due to these unexpected, complicating factors the carbon-capturing potential of the bio-ink could not yet be determined during this research project.

Finding a suitable method to study the livingness of the material was done in several steps. Due to the opaqueness of the material, inverted optical microscopy and 3D-LSM proved unsuitable techniques to study these properties. Chlorophyll extraction also resulted in a dead end as the material's composition is too complex. Ultimately, the autofluorescence of chlorophyll within the algal cells was found to be the only way to study the livingness properly. The images acquired from this test show that algae growth and proliferation are more pronounced on the exterior than within the sample's interior.

5.2 Recommendations

Future research should delve deeper into the CO_2 release patterns of the bio-ink, exploring whether this phenomenon occurs in older samples or those containing algae. This will help answer the question of whether the increase in CO_2 indeed offsets the benefits of photosynthetic activity. Further studies are needed to assess the impacts of environmental factors such as humidity, light cycles, and seasonal variations on the photosynthetic activity and livingness of the material. Understanding these influences is essential for optimizing the overall performance of the ELM. Furthermore, conducting a comparative study to determine if the algae integrated into the ELM exhibit higher photosynthetic activity than traditional plants (e.g. a succulent) might shed light on the benefits of using algae in material design. Lastly, an assessment of the impact of alternative 3D print shapes on photosynthetic activity may uncover more efficient designs.

Further exploration into the behaviour of algae within the samples is necessary to understand aspects such as propagation and proliferation. CLSM would be a good technique for this and will most likely provide insights into the growth

dynamics and livingness of the algae material over time.

Next to this, shrinkage remains a significant challenge, this will most likely play a role in open environments. Research aimed at mitigating shrinkage can expand the material's application possibilities. Transitioning towards application-oriented research by exploring alternative materials or fabrication protocols, potentially beyond 3D printing, could boost this research in the right direction.

As a last comment, implementing measures to reduce plastic waste generated during laboratory work will enhance sustainability practices within the research environment and aligns with the broader ecological goals of this research.

Acknowledgements

I would like to express my heartfelt gratitude to the following individuals, who have played significant roles in my academic journey and the successful completion of this research project.

Firstly, I would like to extend my deepest appreciation and respect to Vivian Vriend for her invaluable guidance and collaboration throughout this project. Our joint efforts in various experiments, including the rheology experiments, greatly contributed to the research. Her camaraderie and insightful conversations were instrumental in making the first half of this research enjoyable and productive.

I want to express my gratitude to Marie-Eve Aubin-Tam, for providing the opportunity to collaborate with all the people in the material design network, this truly enriched my research journey. The time she made for me to help me during my project was one that fit with my wishes and for that I am thankful. I am sincerely appreciative of the opportunities their role as the PI has provided for growth, not only in my academic pursuits but also in navigating the intricate dynamics of research collaborations. Working at the Aubin-Tam Lab has been a memorable chapter in this academic odyssey, one that has contributed in its own distinct way to the tapestry of my learning experience. I would also like to thank Caroline Wehrmann, Timon Idema, Kunal Masania and Marie-Eve Aubin-Tam for taking the time to read my report and guaranteeing the scientific fidelity of this research project, and taking seat in the committee for my defence.

I am indebted to Srikkanth Balasubramanian for his mentorship and unwavering support. His unique perspective on science, coupled with his role as my daily supervisor during his availability, made a profound impact. His encouragement and sense of humour were a constant source of motivation.

I extend my sincere thanks to Roland Kieffer for his boundless energy, his expertise in electronics and chemistry and for providing the necessary setups for the photosynthetic activity measurements. His contributions were essential to the success of this project. To Satya Ammu I am grateful for his collaboration on the overhang test and for navigating the challenges of working with the complex microscope software. Our coffee breaks and engaging discussions on 3D printing and material design were much appreciated and gave me a well-deserved break after many experimental hick-ups. Jeremie Capoulade's assistance with imaging using the CLSM during the challenges of the Covid-19 pandemic and providing raw data for samples requiring imaging were significant contributions to this work. And a special thanks to Jeong-Joo Oh, for his eagerness to delve into the

material when introduced to the lab and for his dedication during the transition period.

Kunal Masania's expertise and enthusiasm were invaluable to this research. I am thankful for the opportunity to work in his lab as if I was part of his team and for his daily check-ins to monitor progress and discuss results. I would like to express my appreciation to Ramon van der Valk for his infinite jokes and also for his assistance in the lab of course. His presence always brightened the research environment. Special thanks to Jan Wingand and Anke Amweg-Welter for their flexibility in autoclaving the inks on a weekly basis, ensuring that there was a never-ending flow of available inks.

I extend my gratitude to Timon Idema for his support throughout my university journey. Tanja Hilkhuisen's guidance and support as a student counsellor were invaluable during my academic career and I know for sure she will provide the right support for many more Nanobiology students in the future.

To my parents, your unwavering support, advice, and comforting hugs have been my anchor through thick and thin. I am profoundly grateful for your love and encouragement. To my siblings, thank you for your expert opinions and for joining me on my two graduation days. Your presence means the world to me. I want to acknowledge my roommates, Tijn and Joris, for the laughter and positivity they brought, especially during these final stages of my project. Last, but certainly not least, to my friends, thank you for your patience as I embarked on this academic journey. I look forward to reconnecting and spending more time together now that this decade of studying has come to a close.

Bibliography

[1] Setter, R. O., Franklin, E. C. & Mora, C. Co-occurring anthropogenic stressors reduce the timeframe of environmental viability for the world's coral reefs. *PLOS Biology* **20**, e3001821 (2022).

[2] Dawson, T. P., Jackson, S. T., House, J. I., Prentice, I. C. & Mace, G. M. Beyond Predictions: Biodiversity Conservation in a Changing Climate. *Science* **332**, 53–58 (2011).

[3] Rockström, J. *et al.* A safe operating space for humanity. *Nature* **461**, 472–475 (2009).

[4] Azoulay, D. *et al.* Plastic & Health: The Hidden Costs of a Plastic Planet. Tech. Rep., CIEL (2019).

[5] Meinshausen, M. *et al.* Greenhouse-gas emission targets for limiting global warming to 2 °C. *Nature* **458**, 1158–1162 (2009).

[6] Walker, M. & Humphries, S. 3D Printing: Applications in evolution and ecology. *Ecology and Evolution* **9**, 4289–4301 (2019).

[7] Suárez-Castro, A. F. *et al.* Global forest restoration opportunities to foster coral reef conservation. *Global Change Biology* **27**, 5238–5252 (2021).

[8] Moreira, D. & Pires, J. C. M. Atmospheric CO2 capture by algae: Negative carbon dioxide emission path. *Bioresource Technology* **215**, 371–379 (2016).

[9] Maharjan, S. *et al.* Symbiotic Photosynthetic Oxygenation within 3D-Bioprinted Vascularized Tissues. *Matter* **4**, 217–240 (2021).

[10] Malik, S. *et al.* Robotic Extrusion of Algae-Laden Hydrogels for Large-Scale Applications. *Global Challenges* **4**, 1900064 (2020).

[11] Zhao, S., Guo, C., Kumarasena, A., Omenetto, F. G. & Kaplan, D. L. 3D Printing of Functional Microalgal Silk Structures for Environmental Applications. *ACS Biomaterials Science & Engineering* **5**, 4808–4816 (2019).

[12] Vriend, V. 3D printing living materials: Optimizing the longevity and photosynthetic ability of microalgae structures (2021).

[13] UN Environment Programme. Visual Feature — Beat Plastic Pollution (2022). URL `http://unep.org/interactive/beat-plastic-pollution/`.

[14] Brandon, J. A., Freibott, A. & Sala, L. M. Patterns of suspended and salp-ingested microplastic debris in the North Pacific investigated with epifluorescence microscopy. *Limnology and Oceanography Letters* **5**, 46–53 (2020).

[15] Li, S. *et al.* Influence of polystyrene microplastics on the growth, photosynthetic efficiency and aggregation of freshwater microalgae Chlamydomonas reinhardtii. *Science of The Total Environment* **714**, 136767 (2020).

[16] Nguyen, P. Q., Courchesne, N.-M. D., Duraj-Thatte, A., Praveschotinunt, P. & Joshi, N. S. Engineered Living Materials: Prospects and Challenges for Using Biological Systems to Direct the Assembly of Smart Materials. *Advanced Materials (Deerfield Beach, Fla.)* **30**, e1704847 (2018).

[17] McHugh, D. *A Guide to the Seaweed Industry* (FAOFISHERIESTECHNICALPAPER, Australia, 2003).

[18] Mohan Bhasney, S., Kumar, A. & Katiyar, V. Microcrystalline cellulose, polylactic acid and polypropylene biocomposites and its morphological, mechanical, thermal and rheological properties. *Composites Part B: Engineering* **184**, 107717 (2020).

[19] Fouad, H. *et al.* Characterization of Microcrystalline Cellulose Isolated from Conocarpus Fiber. *Polymers* **12**, 2926 (2020).

[20] Rodrigo-Navarro, A., Sankaran, S., Dalby, M. J., Del Campo, A. & Salmeron-Sanchez, M. Engineered living biomaterials. *Nature Reviews Materials* **6**, 1175–1190 (2021).

[21] Gilbert, C. *et al.* Living materials with programmable functionalities grown from engineered microbial co-cultures. *Nature Materials* **20**, 691–700 (2021).

[22] Gantenbein, S. *et al.* Three-dimensional printing of mycelium hydrogels into living complex materials. *Nature Materials* **22**, 128–134 (2023).

[23] Moser, F., Tham, E., González, L. M., Lu, T. K. & Voigt, C. A. Light-Controlled, High-Resolution Patterning of Living Engineered Bacteria Onto Textiles, Ceramics, and Plastic. *Advanced Functional Materials* **29**, 1901788 (2019).

[24] Balasubramanian, S., Yu, K., Meyer, A. S., Karana, E. & Aubin-Tam, M. E. Bioprinting of Regenerative Photosynthetic Living Materials. *Advanced Functional Materials* **31** (2021).

[25] Field, C. B., Behrenfeld, M. J., Randerson, J. T. & Falkowski, P. Primary production of the biosphere: Integrating terrestrial and oceanic components. *Science (New York, N.Y.)* **281**, 237–240 (1998).

[26] Chung, I. K., Beardall, J., Mehta, S., Sahoo, D. & Stojkovic, S. Using marine macroalgae for carbon sequestration: A critical appraisal. *Journal of Applied Phycology* **23**, 877–886 (2011).

[27] Guiry, M. D. How Many Species of Algae Are There? *Journal of Phycology* **48**, 1057–1063 (2012).

[28] Parmar, A., Singh, N. K., Pandey, A., Gnansounou, E. & Madamwar, D. Cyanobacteria and microalgae: A positive prospect for biofuels. *Bioresource Technology* **102**, 10163–10172 (2011).

[29] Cabernard, L., Pfister, S., Oberschelp, C. & Hellweg, S. Growing environmental footprint of plastics driven by coal combustion. *Nature Sustainability* **5**, 139–148 (2022).

[30] Fischer, B. B., Wiesendanger, M. & Eggen, R. I. L. Growth condition-dependent sensitivity, photodamage and stress response of Chlamydomonas reinhardtii exposed to high light conditions. *Plant & Cell Physiology* **47**, 1135–1145 (2006).

[31] Timeline - Overview for 3D printing in Publications - Dimensions. URL `https://app.dimensions.ai/analytics/publication/overview/timeline?search_mode=content&search_text=3D%20printing&search_type=kws&search_field=text_search&year_from=1974&year_to=2023`.

[32] Chapman, A. The complete history of 3D printing (2022). URL `https://ultimaker.com/learn/the-complete-history-of-3d-printing/`.

[33] Durbin, D. How much does a 3D printer cost? (2022). URL `https://ultimaker.com/learn/how-much-does-a-3d-printer-cost/`.

[34] Balasubramanian, S., Aubin-Tam, M.-E. & Meyer, A. S. 3D Printing for the Fabrication of Biofilm-Based Functional Living Materials. *ACS Synthetic Biology* **8**, 1564–1567 (2019).

[35] Stender, B., Mantei, W. & Houbertz, R. From Lab to Fab — High-Precision 3D Printing. *Laser Technik Journal* **14**, 20–23 (2017).

[36] Schaffner, M., Rühs, P. A., Coulter, F., Kilcher, S. & Studart, A. R. 3D printing of bacteria into functional complex materials. *Science Advances* **3**, eaao6804 (2017).

[37] Kleger, N., Cihova, M., Masania, K., Studart, A. R. & Löffler, J. F. 3D Printing of Salt as a Template for Magnesium with Structured Porosity. *Advanced Materials* **31**, 1903783 (2019).

[38] Beets], J. Master of Science Nanobiology NB5030 MEP proposal (2021). Non-published.

[39] Xie, B. *et al.* Chlamydomonas reinhardtii thermal tolerance enhancement mediated by a mutualistic interaction with vitamin B12-producing bacteria. *The ISME Journal* **7**, 1544–1555 (2013).

[40] Abu-Ghosh, S., Iluz, D., Dubinsky, Z. & Miller, G. Exogenous Abscisic Acid Confers Salinity Tolerance in Chlamydomonas reinhardtii During Its Life Cycle. *Journal of Phycology* **57**, 1323–1334 (2021).

[41] Zaki, S., Steinwachs, M., Sharifi, S., Gerber, E. & Kahl, R. Oxidation of Tris and formaldehyde to CO2 by neutrophil oxidants. *Research Communications in Molecular Pathology and Pharmacology* **93**, 79–87 (1996).

[42] Wu, Y., Levons, J., Narang, A. S., Raghavan, K. & Rao, V. M. Reactive Impurities in Excipients: Profiling, Identification and Mitigation of Drug–Excipient Incompatibility. *AAPS PharmSciTech* **12**, 1248–1263 (2011).

[43] Kukrety, A., Singh, R. K., Singh, P. & Ray, S. S. Comprehension on the Synthesis of Carboxymethylcellulose (CMC) Utilizing Various Cellulose Rich Waste Biomass Resources. *Waste and Biomass Valorization* **9**, 1587–1595 (2018).

[44] Rizan, C., Bhutta, M. F., Reed, M. & Lillywhite, R. The carbon footprint of waste streams in a UK hospital. *Journal of Cleaner Production* **286**, 125446 (2021).

Appendix A

Mechanical Testing

A.1 Rheology Testing

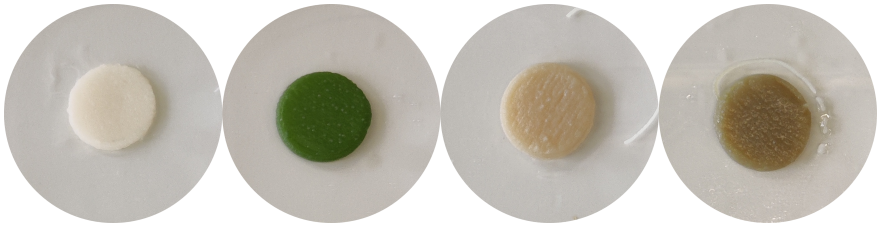

Figure A.1: 7-day-old rheology samples. From right to left: the original bio-ink, bio-ink with algae, gelatin bio-ink and gelatin bio-ink with algae.

A.2 Overhang Testing

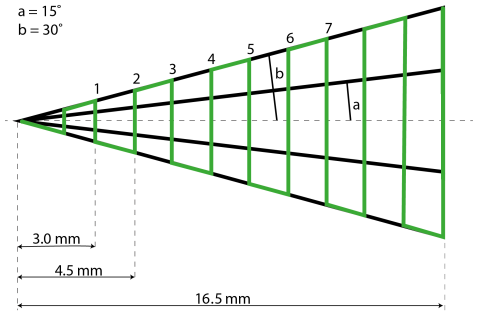

Figure A.2: The dimensions of the overhang print to test the sagging behaviour of the material.

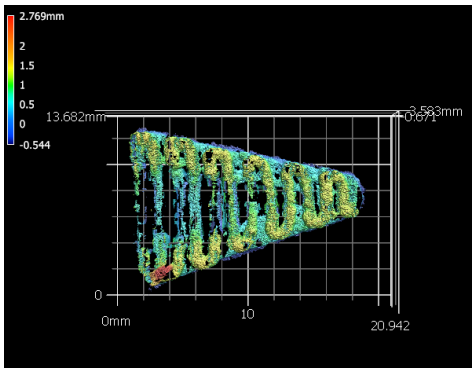

Figure A.3: Top view topographical image of the overhang print.

Appendix B

Livingness Analysis

B.1 Algae Bio-Ink Livingness

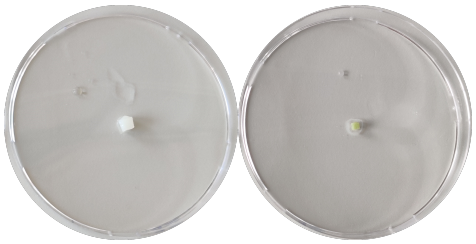

Figure B.1: 6x6x6 layered samples with algae. Crosslinked with 0.2 M $CaCl_2$ for 10 minutes. From left to right: 0-day-old sample and 6-day-old sample.

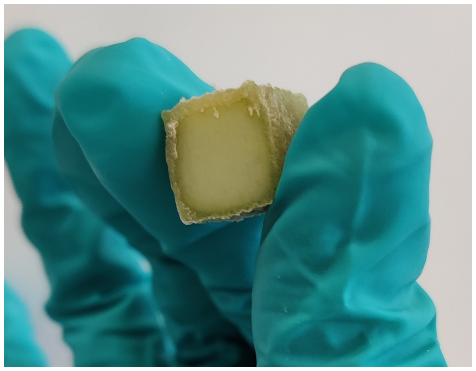

Figure B.2: Bottom of a 14-day-old sample with algae. Crosslinked with 0.2 M $CaCl_2$ for 5 minutes.

B.2 CLSM Imaging Preparation

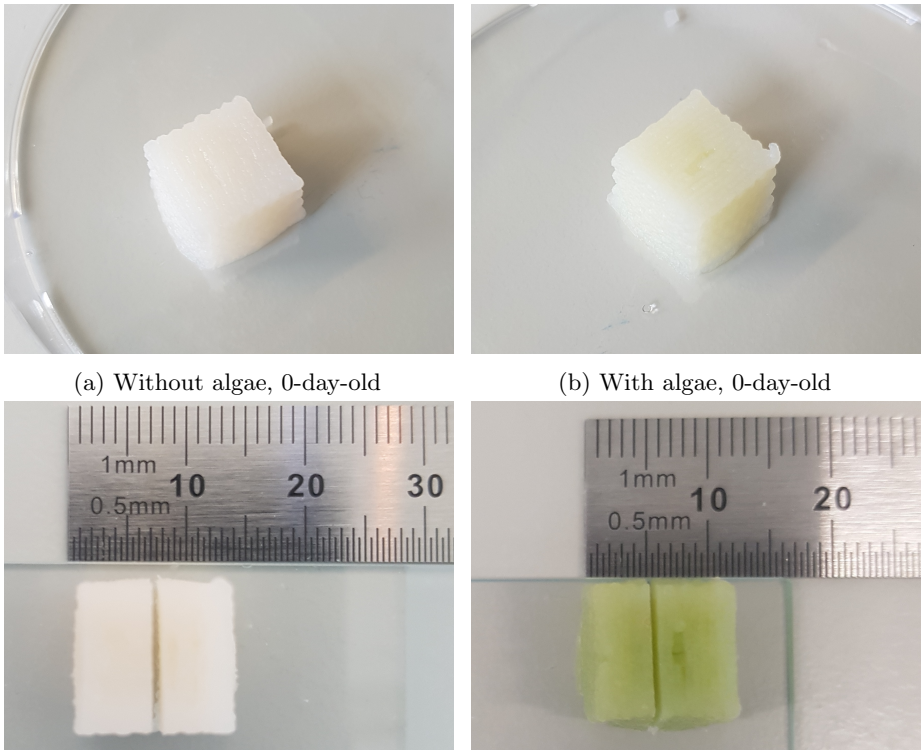

(a) Without algae, 0-day-old

(b) With algae, 0-day-old

(c) Without algae, 7-day-old

(d) With algae, 7-day-old

Figure B.3: CLSM imaging samples, crosslinked with 0.2 M $CaCl_2$ for 5 minutes.

B.3 CLSM Anomalies

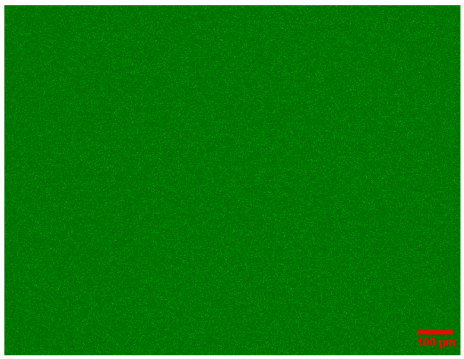

Figure B.4: Day 0, vertical cross-section of a sample with algae.

Appendix C

PA Setups & Extra Results

C.1 Setup 1

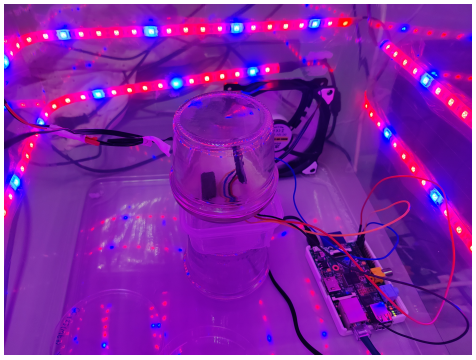

Figure C.1: First setup to measure CO_2, humidity, temperature and light.

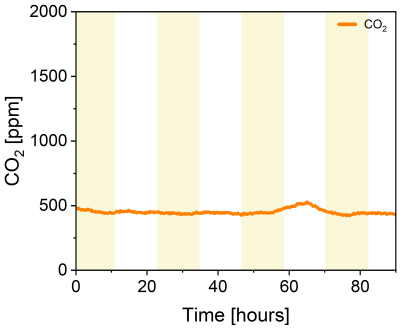

(a) CO_2 level in empty jar

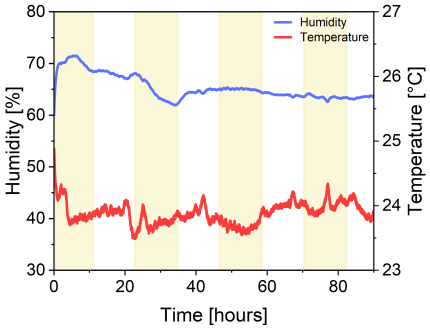

(b) Hum. and temp. in empty jar

Figure C.2: Measurements inside an empty Setup 1, measured over four days.

C.2 Setup 2

Figure C.3: Second setup to measure CO_2, O_2, humidity, temperature and light.

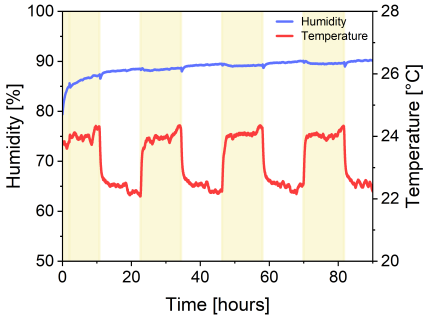

Figure C.4: Humidity and temperature levels measured in the second setup containing a 3D printed algae sample, measured over 4 days.

C.3 Setup 3

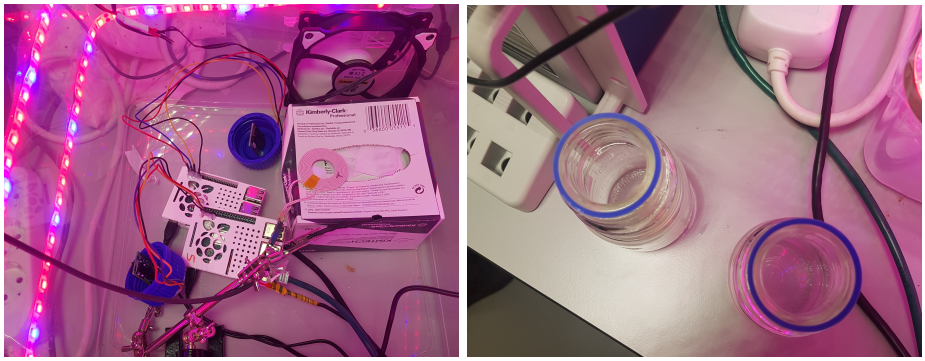

(a) (b)

Figure C.5: Third setup consisted of a laboratory bottle with a blue screw-on lid.

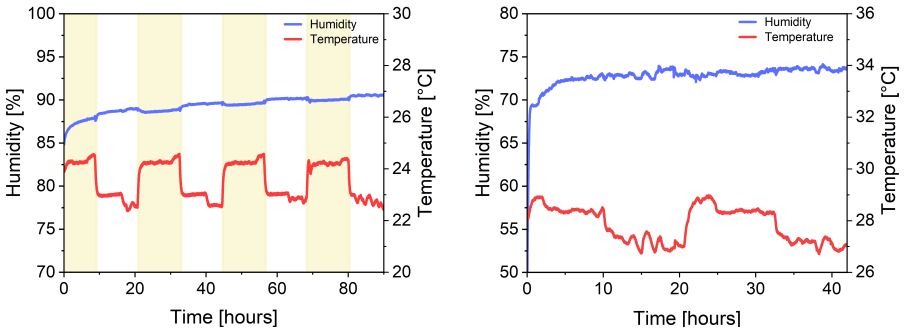

(a) (b)

Figure C.6: Humidity and temperature measurements of (a) the 3D printed bio-ink without algae and (b) the non-autoclaved Tris and MCC mixture.

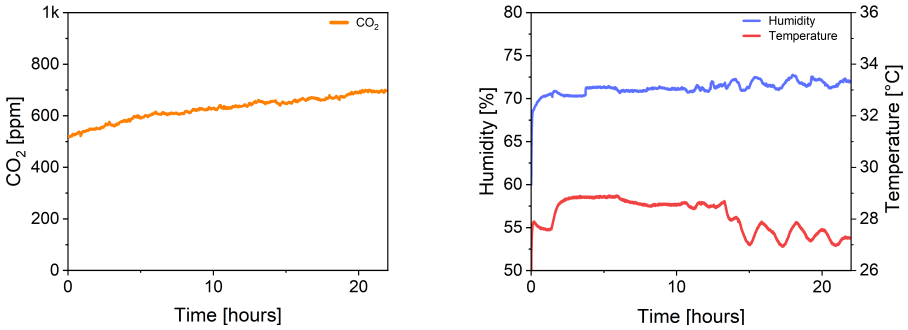

(a) (b)

Figure C.7: CO_2 release of H_2O, measured over 1 day.

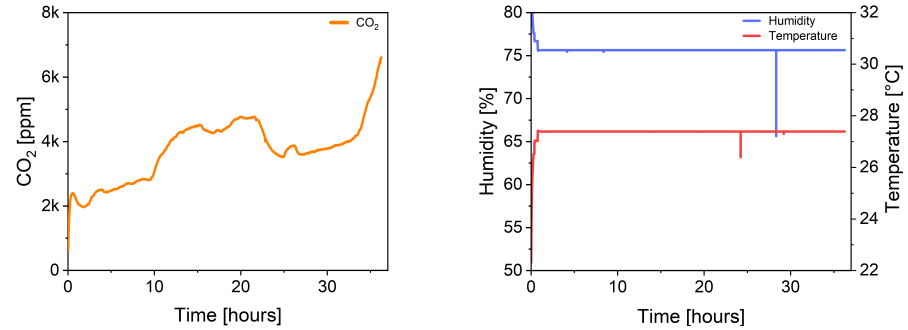

(a) (b)

Figure C.8: CO_2 release of the autoclaved Tris and MCC mixture, measured over 36 hours.

C.4 Setup 4

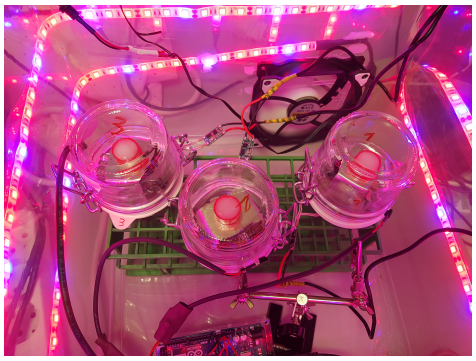

Figure C.9: Fourth setup to measure CO_2, humidity, temperature and light in three jars simultaneously.

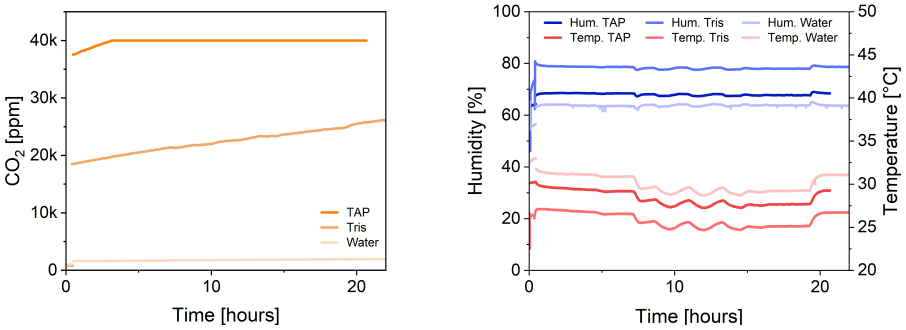

(a) (b)

Figure C.10: Measurements over 1 day of MCC with H2O, Tris or TAP as a media. All samples were non-autoclaved and weighed 5 g.

C.5 Setup 5

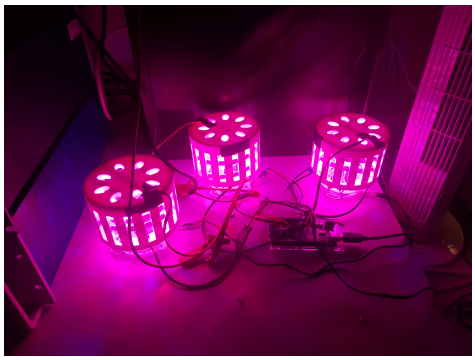

Figure C.11: Fifth setup to measure CO_2, humidity, temperature and light in three jars simultaneously.

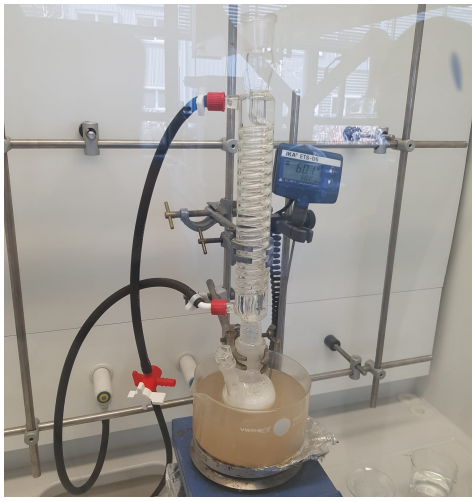

Figure C.12: The treatment of MCC with Hydrazine Monohydrate.

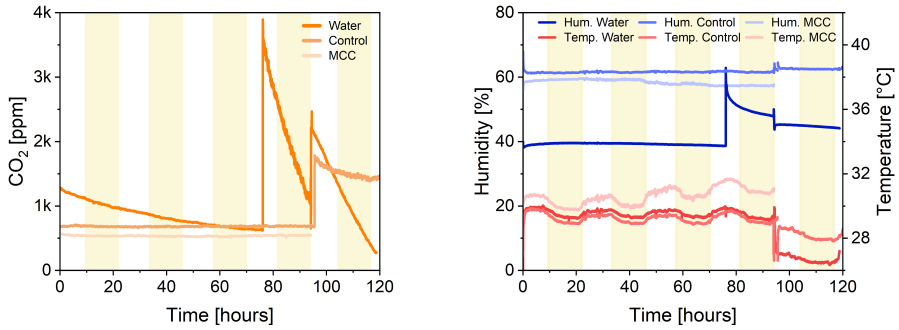

(a) (b)

Figure C.13: Water (device 1), control (device 2) and MCC powder (device 3) test with a subsequent leakage test of jars 1 and 2, measured over 120 hours.

Figure C.14: Fifth setup to measure CO_2, humidity, temperature and light in three jars simultaneously, each with its separate climate control fan.

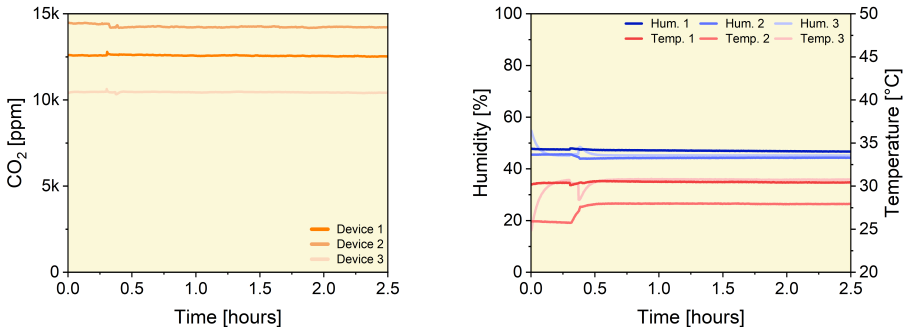

(a) (b)

Figure C.15: Leakage test of jars with added fans, measured over 2.5 hours.

Appendix D

Sample Contaminations

D.1 FungiGate

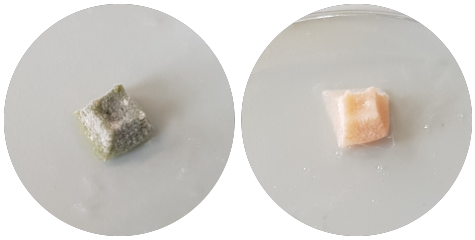

Figure D.1: Samples from one of the three experiments that got contaminated during the 3D printing step. Samples were printed on the 23^{rd} of December 2021, the pictures were taken on the 6^{th} of January 2022.

D.2 Extra Contaminations

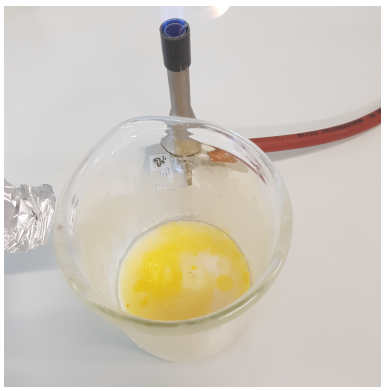

Figure D.2: Three-week-old discarded bio-ink for the MCC age test.